Effects of carnosine supplementation on markers for the pathophysiological development of metabolic dysfunction-associated steatotic liver disease in a diet-induced model

Núbia Alves Grandini[a*], Mariane Róvero Costa[a], Cristina Schmitt Gregolin[a], Juliana Silva Siqueira[a], Taynara Aparecida Vieira[a], Artur Junio Togneri Ferron[b], Fabiane Valentini Francisqueti-Ferron[b], Guilherme Ribeiro Romualdo[a], Ana Lúcia dos Anjos Ferreira[a], Giancarlo Aldini[c], Camila Renata Corrêa[a], Fernando Moreto[a].

[a] São Paulo State university (UNESP), Medical School, 18618687 Botucatu, Brazil
[b] Integrated Colleges of Bauru (FIB), 17056-100, Brazil
[c] Department of Pharmaceutical Sciences, University of Milan, 20133 Milan, Italy

*Corresponding author

Núbia Alves Grandini, Botucatu Medical School, São Paulo State University (UNESP), Professor Montenegro Avenue, Botucatu, 186186687, Brazil. E-mail address: nubia.grandini@unesp.br

Abstract

Consumption of diets high in sugar and fat is related to the development of Metabolic dysfunction-associated steatotic liver disease (MASLD). Carnosine (CAR) is a dipeptide with antioxidant and anti-inflammatory action and has been studied for treating diseases. This work aimed to evaluate the effects of CAR on diet-induced MASLD in rats. Male Wistar rats were distributed into 2 groups (17 weeks): normocaloric (Co, n=12), and hypercaloric diet rich in lipids and simple carbohydrates (MASLD, n=12). After, the animals were redistributed to begin the treatment with CAR (4 weeks): Co (n=6), Co + CAR (n=6), MASLD (n=6), and MASLD + CAR (n=6), administered intraperitoneally (250mg/kg). Evaluations included nutritional, hormonal and metabolic parameters; hepatic steatosis, inflammatory and oxidative markers. MASLD group had a higher adiposity index, systolic blood pressure, glucose, plasma and liver triglycerides and cholesterol, insulin, hepatic steatosis, oxidative markers, and lower PPAR-α (Peroxisome Proliferator-activated receptor α), compared to the Co. CAR attenuated plasma and hepatic triglyceride and cholesterol levels, hepatic steatosis, CD68+ macrophages, and hepatic oxidative markers, in addition to increasing HDL cholesterol levels and PPAR-α, compared to the untreated MASLD group. CAR acts in importants pathophysiological processes of MASLD and may be a therapeutic compound to control the disease.

Keywords: Metabolic dysfunction-associated steatotic liver disease, carnosine, obesity, hypercaloric diet.

1. Introduction

Non-alcoholic fatty liver disease (NAFLD) is the most common liver injury, which affects about a third of the world's population and is defined by the accumulation of fat in liver tissue without alcohol consumption and other liver damage (Younossi et al., 2016). In 2023, a new terminology and definition were proposed, starting to be called Metabolic dysfunction-associated steatotic liver disease (MASLD). Therefore, the MASLD is based on hepatic steatosis with one of the five cardiometabolic risk factors: overweight or obesity, type 2 diabetes mellitus or hyperglycemia, hypertension or antihypertensive drug treatment, and dyslipidemia (Rinella et al., 2023).

MASLD has a spectrum of evolution from simple steatosis and can involve Metabolic disfunction-associated steatohepatitis (MASH) and even liver cancer (Carneros et al., 2020; Francisqueti-Ferron et al., 2022; Rinella et al., 2023). According to a survey based on data from Europe, North America, and Asia, the prevalence of patients with MASLD is around 39% (Lim et al., 2021), while MASH affects around 5% of the world's population (Younossi et al., 2016). Its pathogenesis is still not well defined, but there are two theories for its development: the first is the "two hits" theory, where it is believed that the first aggression is the imbalance caused by insulin resistance (IR) between the hepatic pathways of acquisition and elimination of lipids, and the second attack involves the processes of inflammation and oxidation (Day and James, 1998). The second theory is that its development takes place from a "multiple hits" model, where several aggressive agents trigger this injury, being genetic, epigenetic, nutritional, and inflammatory, including changes in the microbiota, IR, and oxidative stress (Buzzetti et al., 2016; Day and James, 1998).

The Western diet, rich in simple carbohydrates and fats, is a crucial precursor factor of MASLD, which can cause harmful effects on the liver by accumulating these macronutrients (Rives et al., 2020; Vancells Lujan et al., 2021). Data in the literature indicate that women who consume a diet high in sugar and fat have a 119% greater risk (OR, 2.19; 95% CI, 1.40–3.46) of developing fatty liver disease (Jia et al., 2015); similar data were found for adolescents aged 17 years who had the same Western diet consumption pattern (Oddy et al., 2013). The accumulation of fatty acids in the liver generates hepatic steatosis. It favors the excessive production of ROS (reactive oxygen species), causing an imbalance in the antioxidant system and, consequently, oxidative

stress, which can cause various cellular damage (Arroyave-ospina et al., 2021; Yki-Järvinen et al., 2021).

Given the complexity of MASLD and its consequences, the search for forms of prevention and treatment is necessary. Currently, there is no specific pharmacological treatment for this disease, only drugs that treat specific metabolic alterations, such as dyslipidemia and hyperglycemia, are used (Nassir, 2022; Salvoza et al., 2022). On the other hand, the search for bioactive compounds that can be used to improve these conditions emerges, and one of these compounds is carnosine (CAR), a natural dipeptide composed of β-alanine and L-histidine, which can be found in the human body, in higher concentrations in skeletal muscle and brain (Aldini et al., 2021).

For many years CAR was the focus of studies only related to improving the performance of physical exercises, mainly due to its buffering capacity in the muscles (Matthews et al., 2019). However, CAR has been identified as a potential therapeutic agent in treating diseases due to its antioxidant, anti-inflammatory, and ROS-sequestering activity (Chmielewska et al., 2020). Some studies demonstrated that CAR was able to attenuate the development of type 2 diabetes in ob/ob mice (Albrecht et al., 2017), improve parameters related to metabolic syndrome induced by diet in Wistar rats (Al-Sawalha et al., 2019), as well as improve hepatic steatosis in mice that consumed a high-fat diet (Mong et al., 2011) and in a model of type 2 diabetes in db/db mice (Schwank-Xu et al., 2021). Faced with the need to clarify the biological effects of CAR and the scarcity of studies relating this dipeptide to MASLD, the present study aimed to verify the effects of CAR supplementation on markers of the MASLD pathophysiology induced by diet in rats.

2. Material and Methods

2.1. Animals and Experimental Protocol

This study was approved by the Ethics Committee on Animal Use (nº 1322/2019). It was carried out following the Guide for the Care and Use of Laboratory Animals published by the U.S. National Institutes of Health. Male Wistar rats from the Central Animal Facility of the Faculty of Medicine of Botucatu, approximately 21 days old, were kept in individual cages in an environment with temperature (24±2ºC), humidity (55±5%) and light (light cycle-dark 12h) controlled. Initially, they were distributed into two experimental groups, fed different diets for MASLD induction: normocaloric (n=12) and hypercaloric rich in sugar and fat (n=12). On the 17th week, after the difference between plasma triglycerides, defined as an inclusion criterion, the animals were redistributed into

four groups for treatment: a control group that continued receiving the normocaloric diet (co, n=6), a control group that received the normocaloric diet treated with carnosine (Co+CAR, n=6), a group that continued receiving the hypercaloric diet (MASLD, n=6) and a group that received the hypercaloric diet treated with carnosine (MASLD+CAR, n= 6), for four weeks. Feed and water were offered ad libitum. The animals that received the hypercaloric diet also received sucrose in their drinking water at a concentration of 25% throughout the experiment. Both diets were produced according Francisqueti et al. (2017), and are described in Table 1. The groups received CAR supplementation (250 mg/kg/day) or vehicle (sterile saline solution, 0.9% NaCl) intraperitoneally for four weeks. At the end of the 21 weeks, the animals fasted for 8 hours and then were anesthetized (Thiopental 120 mg/kg/i.p.) and euthanized by decapitation. Blood samples, adipose tissue, and liver were collected.

Table 1. Diet composition and nutritional values.

Components	Normocaloric	Hypercaloric
Soybean meal (g/kg)	335	340
Sorghum (g/kg)	278	80
Soy hulls (g/kg)	188,5	116,7
Dextrin (g/kg)	146,5	20
Maize starch (g/kg)	278	80
Sucrose (g/kg)	-	80
Fructose (g/kg)	-	180
Soybean oil (g/kg)	23	-
Lard (g/kg)	-	154,3
Minerals (g/kg)	25	25
Salt (g/kg)	4	4

2.2. Carnosine Supplementation

CAR (L-carnosine) was administered intraperitoneally (250 mg/kg) for four weeks after induction. The dose was defined based on studies where CAR presented effective results and did not generate toxic and/or adverse effects on the animals (Aydın et al., 2017; Kalaz et al., 2016). The infusion was performed using a 30G needle, with a liquid volume close to 500 µL being injected. The product CarnoPureTM (Flamma S.p.A., Chignolo d'Isola, Bergamo, Italy) was used exclusively for scientific experiments and used in studies abroad. This product was kindly provided by this company, free of charge, for carrying out this experiment.

2.3. Nutritional characterization and obesity

Nutritional characterization was evaluated based on feed, water, and caloric intake (feed and water). Food and water intake were calculated daily from the individual leftovers of each animal. Caloric intake was calculated through food intake multiplied by the energy value of each diet. The characterization of obesity was based on weight gain and adiposity index. Weight gain was calculated by the difference between the final weight and the initial weight of the animals [weight gain (g)=final weight (g) - initial weight (g)]. The adiposity index represents the ratio between the sum of fat deposits (visceral, epididymal, and retroperitoneal) and the final weight of the animals (adiposity index = sum of fat deposits (g)/final weight (g) x 100) (Costa et al., 2019).

2.4. Systolic Blood Pressure

Systolic blood pressure (SBP) was measured by the indirect method of tail plethysmography using an electric sphygmomanometer Narco Bio-System® PE 300, model 709-0610 (International Biomedical, Inc, Houston, Texas, USA). For this purpose, the animals were kept for 5 minutes in a wooden box heated between 38ºC and 40ºC to stimulate arterial vasodilation. Afterward, the cuff was attached to the tail of each animal and inflated (200 mmHg), and deflated, allowing the recording of arterial pulses collected in a Gould RS 3200 polygraph (Gould Instrumenta Valley View, Ohio, USA). The mean of the three PAS readings was recorded for each animal (Siqueira et al., 2022).

2.5. Biochemical and Hormonal Analysis

Glucose was determined using a glucometer (Accu-Check Performa; Roche Diagnostics, Indianapolis, IN, USA). The concentrations of urea, creatinine, uric acid, triglycerides, total cholesterol and its fractions, HDL cholesterol and non-HDL cholesterol (n-HDL) were analyzed by the enzymatic colorimetric method with commercial kits (BioClin®, Belo Horizonte, MG, Brazil) in automated biochemical equipment (Chemistry Analyzer BS-200, Mindray Medical International Limited, Shenzhen, China).

The insulin level was measured using the indirect enzyme immunoassay (ELISA) method using commercial kits (Linco Research Inc., R&D Systems, Millipore, and B-Bridge International Inc.), and the reading was performed on a Spectramax 190 microplate spectrophotometer (Molecular Devices®, Sunnyvale, CA, USA). The IR assessment was performed using the Homeostasis Model Index - Insulin Resistance (HOMA-IR) using glycemia and plasma insulin parameters. The calculation of the HOMA index obeyed the following formula: insulin (µl U/mL) x blood glucose (mmol/L) / 22.5 (Francisqueti-Ferron et al., 2022).

2.6. Liver Tissue Analysis

2.6.1. Histological Parameters

After collection, liver tissue was stored in 4% paraformaldehyde with 0.1M phosphate buffer (pH=7.4) during the first 24 hours. Afterward, the tissue was transferred

to ethyl alcohol, and the samples were embedded in paraffin to obtain five µm-thick sections. Such sections (one per animal) were stained with Hematoxylin & Eosin (HE) and evaluated for steatosis, taking into account the macro and microvesicular aspects, according to the NAFLD Activity Score (NAS) parameter (Liang et al., 2014). Then, ten fields were randomly selected (20x objective), which were evaluated in each section, and the following scores were considered: 0 (<5% of the microscopic field), 1 (5-33%), 2 (33-66%), or 3 (>66%). Other liver samples were frozen and included in an Optimal Cutting Temperature medium (Tissue-Trek, USA), and 10 µm sections were obtained and stained with Oil red (Sigma Aldrich, USA) to obtain representative photos. To assess the presence and deposition of collagen sections samples were stained with picrosirius red with subsequent detection by refringent images on optical microscope. The METAVIR score system was used to evaluate the level of fibrosis: F0: no fibrosis; F1: portal fibrosis without septa; F2: portal fibrosis with septa; F3: septa without cirrhosis; F4: cirrhosis.

2.6.2. Immunohistochemistry for CD68

Other 5 µm thick liver sections were submitted to antigen retrieval in 0.01M citrate buffer (pH 6.0, 120ºC, five min.) in a Pascal pressure chamber (Dako Cytomation, Denmark). After blocking endogenous peroxidase with 10% H2O2 in phosphate-buffered saline (PBS) (15 minutes), the slides were treated with skimmed milk for 60 minutes to block nonspecific binding. Then, the histological sections were incubated in a humid chamber (4ºC overnight) with a primary anti-CD68 antibody solution (macrophages, ab125212, 1:500 dilution, Abcam, UK). Then, the slides were incubated with HRP polymer (Horseradish peroxidase) in a single step (EasyPath - Erviegas, Brazil) (20 minutes at room temperature). The reactions were revealed with the chromogen 3'3-diaminobenzidine (DAB) (Sigma Aldrich, USA), and the slides were counterstained with Harris hematoxylin. CD68+ macrophages were counted in 10 randomly selected fields (20x) and divided by field area (mm²) using Image J software (NIH, USA) (Romualdo et al., 2022).

2.6.3. Oxidative Stress markers

Malondialdehyde (MDA) level was used to assess lipid peroxidation. Briefly, 250 µL of supernatant from hepatic tissue was added to 750 µL of 10% trichloroacetic acid for protein precipitation. The samples were centrifuged (3000 rpm, for 5 minutes; Eppendorf® Centrifuge 5804-R, Hamburg, Germany), and the supernatant was removed. Thiobarbituric acid (ATB) was added at a ratio of 0.67% (1:1), and the samples were heated for 15 minutes at 100°C. After cooling, the reading was performed at 535 nm in the Spectra Max 190 microplate reader (Molecular Devices®, Sunnyvale, CA, USA). The MDA concentration was obtained by the molar extinction coefficient (1.56 x

105 M-1-cm-1) and the absorption of the samples, and the final result was reported in nmol/g of protein (Siqueira et al., 2023).

To quantify protein carbonylation (CBO), 100 µL of liver tissue homogenate was used for 100 µL of 2,4-dinitrophenylhydrazine (DNPH, 10mM in 2M HCl). The samples were incubated for 10 minutes at room temperature, and then 50 µL of sodium hydroxide (6M NaOH) was added and incubated again for 10 minutes at room temperature. Reading at 450 nm was performed on a Spectramax 190 microplate reader (Molecular Devices®, Sunnyvale, CA, USA). The results were obtained by the molar extinction coefficient (22,000 M -1 cm -1) of DNPH and expressed in nmol/g of protein. Protein carbonylation levels were expressed in nmol of DNPH/mg of protein (Garcia et al., 2022).

Advanced oxidation protein products (AOPP) were detected in liver tissue. Tissue samples were homogenized in PBS buffer at 1:10 (sample:PBS). AOPP quantification was performed by diluting 1:5 of 200 µl of the sample (homogenate). 200 µl of Chloramine-T (0-100 umol/L) was used for the calibration curve, and 200 µl of PBS as a blank. 10 µl of 1.16M KI (potassium iodide) and 20 µl of acetic acid were added to the samples. Absorbance was read immediately at 340 nm (Multiskan Ascent spectrophotometer, Labsystems, Vantaa, Finland). The final concentration of AOPP is expressed in chloramin units (umol/L), and the result in the liver tissue is corrected for the amount of protein (Ferron et al., 2019).

2.6.4. Hepatic Levels of Triglycerides and Cholesterol

Intracellular levels of hepatic triglycerides and cholesterol were determined by a colorimetric method (Colorimetric Triglycerides and Cholesterol Assay Kit; Cayman Chemical, Ann Arbor, MI, USA). The results were corrected for the amount of tissue (Francisqueti-Ferron et al., 2022).

2.7. Gene Expressions

Gene expression of peroxisome proliferator-activated receptor α (PPAR-α; gene *Ppara*, primers F-AGATGGGCTGGTTCTTCCTC and R-CAGTGCATTTGCCAGG), very long-chain acyl-CoA dehydrogenase (VLCAD, gene *Acadvl*, primers F-ATGGAATTCATGGCCAGTGAGGCCACTC and R-TTTACGAATTCTCAGACTCTAAGGGGGT) and β-actin (gene *Actb*, primers F-GGGAAATCGTGCGTGACAT and R-CAGGAGGAGCAATGATCTT) were performed using real time PCR (polymerase chain reaction). Total RNA (ribonucleic acid) was extracted from liver tissue using the TRIzol® reagent (Invitrogen, Carlsbad, CA, USA) according to the manufacturer's specifications. The RNA was subjected to reverse transcription for conversion to cDNA (complementary deoxyribonucleic acid) (High-Capacity cDNA Reverse Transcription Kit, Applied Biosystems, CA, USA) using the

provided primers (Exxtend Biotecnologia Ltda, Campinas-SP, Brazil). The real-time PCR kit used the cDNA (TagMan® Gene Expression Assays, Applied Biosystems, Foster City, CA, USA) to evaluate expressions. The β-actin was used to normalize expressions of PPAR-α and VLCAD.

2.8. Statistical Analysis

Results are expressed as mean ± standard deviation. Two-way ANOVA determined differences between groups, and data were subjected to Tukey's post hoc test to compare all groups. Histological parameters are expressed as medians, and Kruskal-Wallis was used with Tukey's post hoc test. Statistical analyzes were performed using Sigma Plot 12.0 software for Windows (Systat Software Inc., San Jose, CA, USA). A p-value <0.05 was considered statistically significant and all performed statistical analyzes were tested to ensure the power to detect differences among groups and the sample size.

3. Results

3.1. Nutritional characterization and obesity

The nutritional characterization and obesity is presented in Table 2. It is possible to observe that the MASLD and MASLD+CAR groups had lower food intake, higher water, caloric intake, and more significant weight gain when compared to the Co and Co+CAR groups, respectively. There was no difference in the initial body weight between groups. The MASLD group had a higher final weight when compared to the Co group. The adiposity index determined the presence of obesity, and it can be seen that the MASLD induction groups (MASLD and MASLD+CAR) had higher adiposity indices when compared to the control groups (Co and Co+CAR, respectively).

Table 2. Nutritional characterization and obesity.

	Groups				Effects		
	Co	**Co+CAR**	**MASLD**	**MASLD+CAR**	**Diet**	**CAR**	**Interactions**
Food intake (g/day)	37.0 ± 2.31	36.3 ± 2.07	25.6 ± 0.904*	25.3 ± 1.72†	<0.001	0.528	0.858
Water intake (ml/day)	53.2 ± 3.79	52.0 ± 7.17	68.0 ± 4.02*	64.9 ± 3.48†	<0.001	0.320	0.564
Caloric intake (kcal/day)	133 ± 8.28	130 ± 7.42	166 ± 7.84*	168 ± 5.44†	<0.001	0.849	0.584
Initial body weight (g)	324 ± 25.0	324 ± 26.8	320 ± 16.4	314 ± 27.1	0.450	0.775	0.753
Final body weight (g)	502 ± 57.2	477 ± 25.8	569 ± 38.0*	530 ± 68.5	0.008	0.133	0.743
Weight gain (g)	145 ± 48.9	137 ± 23.2	250 ± 34.6*	198 ± 48.6†	<0.001	0.085	0.201
Adiposity index (%)	4.15 ± 1.60	3.12 ± 1.11	8.51 ± 1.03*	7.68 ± 2.56†	<0.001	0.19	0.883

Data are presented as mean ± standard deviation. Effects are the comparison by two-way ANOVA with Tukey's post-hoc test, with p<0.05 as statistically significance. Co: control group; Co+CAR: control group treated with carnosine; MASLD: MASLD induction group; MASLD+CAR: MASLD induction group treated with carnosine. * vs Co; † vs Co+CAR.

3.2. Systolic Blood Pressure

Figure 1 shows the Systolic Blood Pressure (SBP) levels. The MASLD group had a higher SBP compared to the Co group.

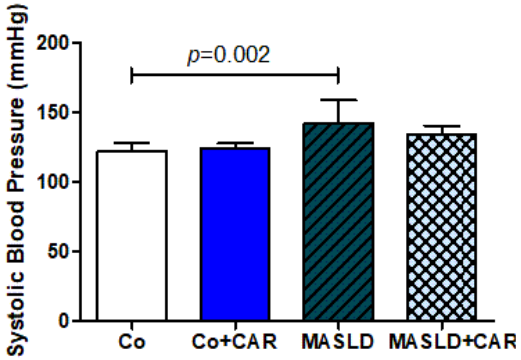

Figure 1. Systolic Blood Pressure Levels. Data are presented as mean ± standard deviation. Comparison by two-way ANOVA with Tukey's post-hoc test. p<0.05 statistically significant. Co: control group; Co+CAR: control group treated with carnosine; MASLD: MASLD induction group; MASLD+CAR: MASLD induction group treated with carnosine.

3.3. Biochemical and hormonal analysis

Table 3 shows the biochemical and hormonal markers. The MASLD and MASLD+CAR groups had lower urea levels when compared to the Co and Co+CAR groups, respectively. There was no significant difference uric acid, and creatinine. ALT levels were significantly lower in control treated with CAR and MASLD induction groups (MASLD and MASLD+CAR) had higher blood glucose levels when compared to the control groups (Co and Co+CAR, respectively). Co+CAR showed lower concentrations of total cholesterol compared to the Co group, while MASLD+CAR showed higher concentrations of total cholesterol compared to the Co+CAR group. Regarding triglycerides, the MASLD and Co+CAR groups had higher and lower concentrations when compared to the Co group. In contrast, the MASLD+CAR group had lower and higher levels when compared to the MASLD and Co+CAR groups, respectively. In addition, the MASLD+CAR group had higher HDL cholesterol (high-density lipoprotein) levels than the MASLD group. There was no statistical difference for non-HDL cholesterol levels. The MASLD and MASLD+CAR groups had higher insulin and HOMA-IR values when compared to the Co and Co+CAR groups, respectively.

Table 3. Biochemical and hormonal markers.

	Groups				Effects		
	Co	**Co+CAR**	**MASLD**	**MASLD+CAR**	**Diet**	**CAR**	**Interactions**
AST (U/l)	155 ± 34.3	125 ± 18.6	114 ± 21.0	130 ± 32.4	0.128	0.532	0.058
ALT (U/l)	104 ± 14.4	69.5 ± 16.1*	83.0 ± 26.5	87.5 ± 21.5	0.858	0.084	0.028
Uric acid (mg/dl)	0.967 ± 0.175	0.800 ± 0.420	1.27 ± 0.761	1.67 ± 1.69	0.150	0.768	0.476

Urea (mg/dl)	58.8 ± 8.66	61.0 ± 9.63	35.0 ± 15.5*	44.2 ± 4.58†	<0.001	0.195	0.417
Creatinine (mg/dl)	4.48 ± 3.08	4.59 ± 5.01	4.48 ± 1.68	4.36 ± 0.985	0.931	0.998	0.930
Blood Glucose (mg/dl)	78.0 ± 8.29	86.3 ± 11.4	88.8 ± 6.74*	97.3 ± 4.50†	0.004	0.020	0.980
Total Cholesterol (mg/dl)	62.3 ± 7.12	46.5 ± 10.1*	52.7 ± 9.63	62.0 ± 8.32†	0.430	0.380	0.002
Triglycerides (mg/dl)	70.4 ± 16.9	41.0 ± 8.32*	205 ± 34.6*	112 ± 27.4#†	<0.001	<0.001	0.004
HDL (mg/dl)	14.5 ± 3.02	14.0 ± 1.79	11.4 ± 2.33	15.5 ± 3.27#	0.471	0.114	0.047
n-HDL (mg/dl)	47.8 ± 4.67	40.5 ± 10.9	40.2 ± 6.59	46.5 ± 5.79	0.785	0.870	0.035
Insulin (ng/ml)	0.224 ± 0.031	0.175 ± 0.039	0.306 ± 0.039*	0.293 ± 0.073†	<0.001	0.132	0.379
HOMA - IR	1.24 ± 0.199	1.07 ± 0.227	1.93 ± 0.304*	2.03 ± 0.535†	<0.001	0.800	0.342

Data are presented as mean ± standard deviation. Effects are the comparison by two-way ANOVA with Tukey's post-hoc test, with $p<0.05$ as statistically significance. Co: control group; Co+CAR: control group treated with carnosine; MASLD: MASLD induction group; MASLD+CAR: MASLD induction group treated with carnosine; AST: aspartate aminotransferase; ALT: alanine aminotransferase; HDL: high density lipoprotein; n-HDL: non-high-density lipoprotein; HOMA-IR: homeostasis model assessment – insulin resistance. * vs Co; # vs MASLD; † vs Co+CAR.

3.4. Liver Tissue Analysis

3.4.1. Histological Parameters

Figure 2 shows the determination of hepatic steatosis by histological parameters. The MASLD induction group supplemented with carnosine (MASLD+CAR) attenuated the steatosis with macro and microvesicular aspects developed by the untreated MASLD induction group (MASLD). Also, picrosirius red staining demonstrate septal fibrosis deposition (black arrow) in MASLD that is significantly reduced in MASLD treated with CAR.

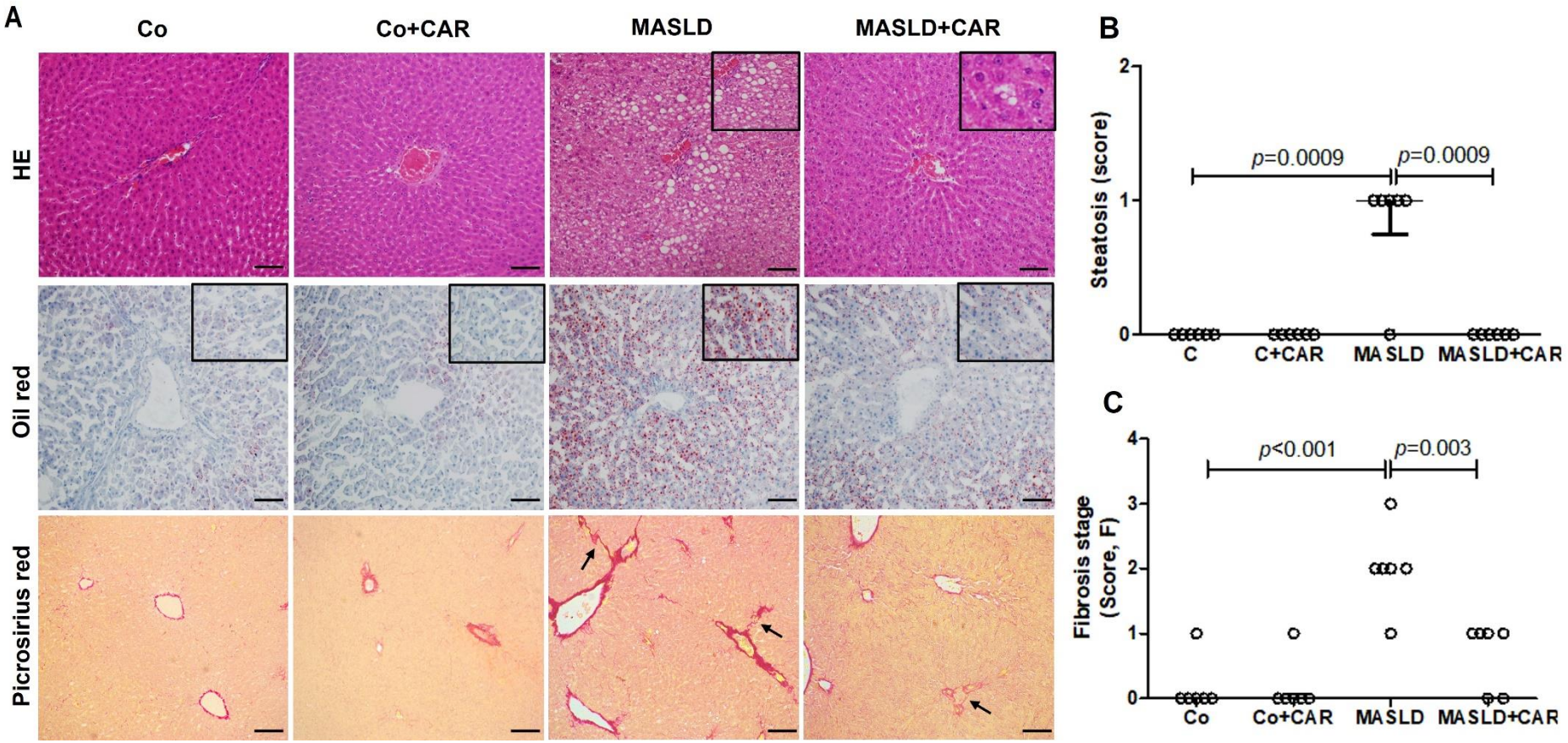

Figure 2. Determination of hepatic steatosis by histological parameters. A) Representative photomicrographs of liver sections stained with HE, Oil red and Picrosirius red (scale bar: 50 µm); B) Steatosis Score; C) Fibrosis Stage. Data are presented as median (max – min) and individual data points, and were analyzed by Kruskal-Wallis with Tukey's post-hoc test. $p<0.05$ statistically significant; n=6 animals/group. Co: control group; Co+CAR: control group treated with carnosine; MASLD: MASLD induction group; MASLD+CAR: MASLD induction group treated with carnosine.

3.4.2. Immunohistochemistry for CD68+

Figure 3 shows the effects of CAR supplementation on the density of CD68+ macrophages. The density of macrophages is lower in the MASLD+CAR group compared to the MASLD group, pointing to an attenuation of the inflammation generated by CAR.

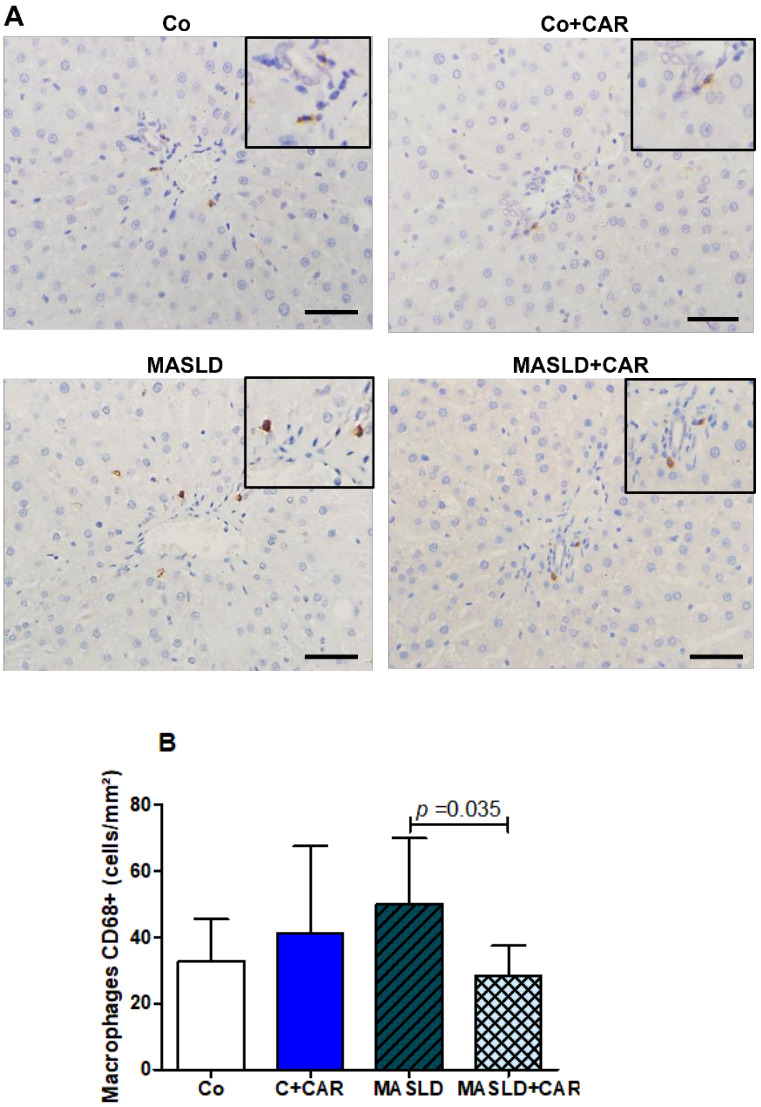

Figure 3. Effects of CAR treatment on CD68+ expression density. A) Representative photomicrographs of immunostained liver sections (details, scale bar: 100 µm). B) Semi-quantitative analysis. Data are presented as mean ± standard deviation ~~and individual data points~~, and were analyzed by two-way ANOVA with Tukey's post-hoc test. $p<0.05$ statistically significant; n=6 animals/group. Co: control group; Co+CAR: control group treated with carnosine; MASLD: MASLD induction group; MASLD+CAR: MASLD induction group treated with carnosine.

3.4.3. Oxidative Stress Markers

Figure 4 shows levels of MDA (Figure 4A), CBO (Figure 4B) and AOPP (Figure 4C) in liver tissue. The MASLD group showed higher levels of MDA, CBO, and AOPP compared to the Co group, and in contrast, the MASLD+CAR group attenuated MDA,

CBO, and AOPP levels compared to the MASLD group. Levels of CBO and AOPP of the MASLD+CAR group are elevated compared to the Co+CAR group.

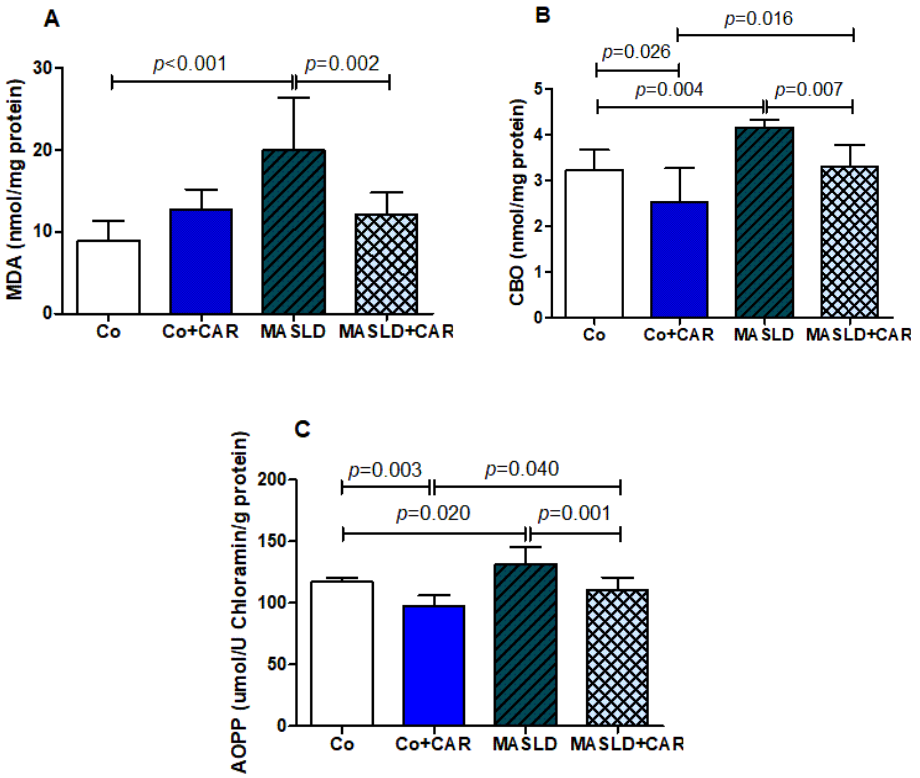

Figure 4. Oxidative Stress Markers. A) Liver levels of MDA; B) Liver levels of CBO; C) Liver levels of AOPP. Data are presented as mean ± standard deviation. Comparison by two-way ANOVA with Tukey's post-hoc test. p<0.05 statistically significant. Co: control group; Co+CAR: control group treated with carnosine; MASLD: MASLD induction group; MASLD+CAR: MASLD induction group treated with carnosine; MDA: Malondialdehyde; CBO: Protein carbonylation; AOPP: Advanced protein oxidation products.

3.4.4. Liver levels of triglycerides and cholesterol

Figure 5 shows the hepatic levels of triglycerides and cholesterol. The MASLD group had higher triglyceride and cholesterol concentrations in the liver than the Co group. The CAR-treated MASLD induction group (MASLD+CAR) had elevated triglyceride concentrations relative to the Co+CAR group but attenuated hepatic triglyceride and cholesterol levels compared to the untreated MASLD induction group.

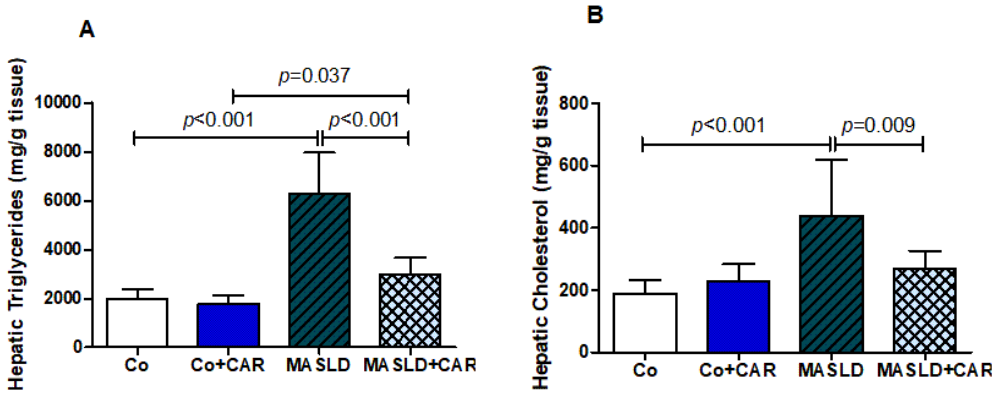

Figure 5. Liver levels of triglycerides and cholesterol. A) Hepatic levels of triglycerides; B) Hepatic cholesterol levels. Data are presented as mean ± standard deviation. Comparison by two-way ANOVA with Tukey's post-hoc test. p<0.05 statistically significant. Co: control group; Co+CAR: control group treated with carnosine; MASLD: MASLD induction group; MASLD+CAR: MASLD induction group treated with carnosine.

3.5. PPAR-α and VLCAD Gene Expressions

Figure 6 shows gene expression by real-time PCR in liver tissue. It can be seen that the MASLD group had lower PPAR-α and VLCAD mRNA levels compared to the Co group. In contrast, the MASLD+CAR group had higher levels of PPAR-α than MASLD group. MASLD+CAR also showed higher VLCAD mRNA levels than MASLD but not enough to get statistical significance.

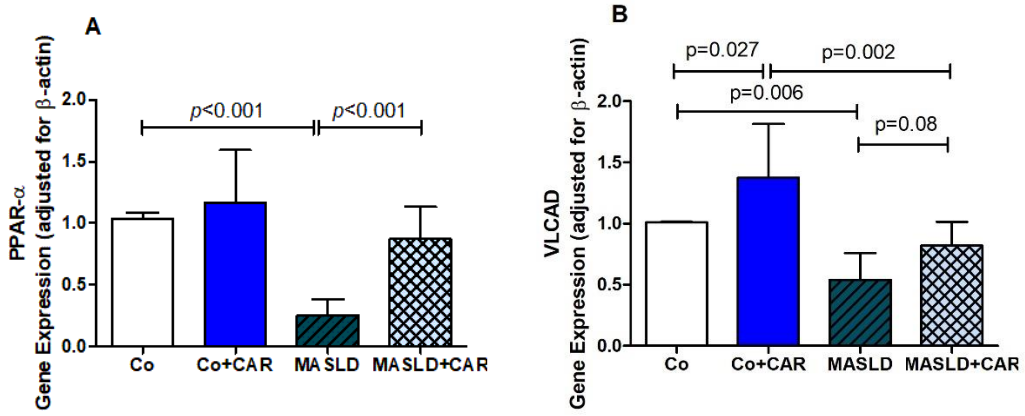

Figura 6. Gene expressions in liver tissue. A) PPAR-α Gene Expression; B) VLCAD Gene Expression. Comparison by two-way ANOVA with Tukey's post-hoc test. p<0.05 statistically significant. Co: control group; Co+CAR: control group treated with carnosine; MASLD: MASLD induction group; MASLD+CAR: MASLD induction group treated with carnosine.

4. Discussion

The present study aimed to verify the effects of CAR supplementation on diet-induced MASLD in rats. Studies have shown that the high consumption of diets rich in sugars and fats, as well as sugary drinks, favors the development of MASLD, a condition

associated with several morbidities, such as metabolic syndrome, insulin resistance, inflammation and oxidative stress (Carneros et al., 2020). In this condition, the present study demonstrated beneficial effects of CAR in the treatment of MASLD by influencing activity of key modulators of lipid metabolism, reflecting in lower lipid deposition and lower inflammatory and oxidative injuries in liver tissue.

MASLD was recently defined by the presence of hepatic steatosis associated with one of the five cardiometabolic risk factors: overweight or obesity, type 2 diabetes mellitus or hyperglycemia, hypertension or antihypertensive drug treatment, and dyslipidemia (Rinella et al., 2023). In this study, the MASLD group presented obesity (higher adiposity index), hypertension, insulin resistance and dyslipidemia, evidencing the presence of the condition. Higher water and caloric intakes were observed in the MASLD group, with a consequent increase in final body weight and weight gain, as observed in other similar studies (Garcia et al., 2022; Siqueira et al., 2022). Although the animals in the MASLD group had lower food intake than the Co group, they had higher sugar-sweetened-water (25% sucrose) consumption, justifying the weight gain and higher final weight of these animals. This dietary habit in association with physical inactivity generates a positive energy balance, which results in hypertrophy and hyperplasia of adipocytes. This change in adipose tissue causes accumulation of fatty acids as well as changes in the production of inflammatory cytokines (Garcia et al., 2019; White and Ravussin, 2019). When hepatocytes reach their lipid-storing capacity, lipotoxicity and hepatocellular stress lead to apoptosis, and then, chemokines are released to activate resident macrophages, kupffer cells, and circulating monocyte-derived macrophages (Li et al., 2020). Macrophages are essential factors in the progression of MASLD. Their activation and proliferation promote several stimuli for inflammatory perpetuation with consequent progression to MASH (Ju and Tacke, 2016). Oxidative stress is also a critical alteration that favors the development of MASLD since the hepatic accumulation of lipids favors the overproduction of ROS, which at high concentrations leads to a decrease in the activity of antioxidant systems, causing several structural and oxidative changes in the metabolism of cellular macromolecules (Bayarsaikhan et al., 2022; Gabbia et al., 2021; Hong et al., 2021). Hepatic storage of triglycerides and cholesterol is an initial mechanism to prevent toxicity; however, excess steatosis can induce lipotoxicity and glucotoxicity in the liver, producing ROS in various organelles (Sabir et al., 2022; Yang and Jo, 2018). Once stablished the pathophysiology of MASLD, the present study aimed to verify the effects of CAR treatment on markers for the development of this condition.

The treatment with CAR did not influence food, water and caloric intake, weight gain, and final weight of the animals in the treated MASLD induction group (MASLD+CAR), corroborating data found in the literature, where CAR supplementation did not influence food and water intake, as well as animal weight parameters (Everaert et al., 2021; Giriş et al., 2014). Treatment with CAR did not influence levels of adiposity index, hypertension, and total cholesterol in the MASLD group. Instead, it was observed attenuated plasma triglyceride levels, as well as improved HDL cholesterol concentrations. Al-Sawalha et al. (2019) conducted a study in rats with metabolic syndrome and CAR supplementation for 16 weeks, where changes similar to those found in our work on the lipid profile were also observed. The positive effects of CAR on lipid parameters were also observed in humans with type 2 diabetes (Houjeghani et al., 2018) who received CAR for 12 weeks, demonstrating that CAR can act as an anti-dyslipidemic agent and may have protective effects in models of obesity-related complications.

The mechanism by which CAR intervenes on lipid profile is not well understood. In the present work, along with a better plasma lipid profile and lower deposition of lipids in liver tissue it was observed important modulatory activity on PPAR-α gene expression. PPAR-α is a key transcription factor that regulates transcription of genes involved in fatty acid β-oxidation and thermogenesis (Todisco et al., 2022). Moreover, in response of PPAR-α activation or not, it was observed a modulatory effect on mRNA expression of VLCAD, an enzyme responsible for the catalysis of the first reaction of the mitochondrial very long chain fatty acids β-oxidation (Koo, 2013). The oxidation of fatty acids, mainly regulated by PPAR-α, reduces the levels of fatty acids available in the liver, using them as an energy source. However, in the face of mitochondrial dysfunction, the β-oxidation process is impaired, thus generating fat accumulation, as well as the production of ROS (Arroyave-ospina et al., 2021; Chen et al., 2020; Mong et al., 2011). In the present study, the MASLD group showed lower PPAR-α gene expression than the Co group. CAR supplementation in the MASLD+CAR increased mRNA levels compared to the MASLD group, pointing to a possible role on this component. Additionally, mRNA levels of VLCAD showed similar behavior, demonstrating high response in Co+CAR and a restoring effect in the MASLD+CAR, even still not statistically significant. There are no data in the literature reporting the role of CAR on PPAR-α, but there are studies where β-alanine, a precursor of CAR, was able to stimulate the expression of PPAR-β/δ, a key regulator of muscle lipid balance, suggesting that histidyl dipeptides can be natural ligands of PPARs (Schnuck et al., 2016). In line with this, these findings suggest a possible role of CAR on dysfunctions of lipid metabolism, in view of the reduction of

plasma and hepatic triglycerides, hepatic cholesterol, steatosis and oxidative stress, as well as an increase in PPAR-α gene expression in MASLD.

Although no significant difference was observed between the MASLD group and the Co group for CD68 expression, CAR significantly attenuated their activation compared to the MASLD group. The reduction of macrophage infiltration in MASLD+CAR is in line with the reduction of collagen deposition marked by Sirius red staining and fibrosis score in the same group, suggesting a possible role of CAR in the atenuation of MASLD progression to MASH. Similar data were found in the literature, where CAR attenuated inflammatory infiltrates (monocytes and macrophages) (Chen et al., 2017). Another study reported a significant decrease in CD68 macrophages in mice with atherosclerotic lesions treated with CAR (Barski et al., 2013). CAR's action on macrophages may be related to its potential to reduce oxidative stress, which is directly related to inflammation. However, CAR may also be acting on MIF, generating a decrease in the activity of CD68 macrophages in the obesity model. Aiello et al., 2022 observed that CAR increased MIF in a 3D skin model, associating this effect with the antioxidant action of CAR and its power to reduce oxidative stress and its positive effect on aging.

In line with this hypothesis, the present work showed that the MASLD group had higher hepatic levels of MDA, carbonyl proteins (CBO), and AOPP in comparison to the control group, but, the treatment with CAR (MASLD+CAR group) attenuated the hepatic concentrations of MDA, CBO, and AOPP in comparison to the MASLD group. It is also possible to notice lower concentrations of CBO and AOPP in the Co+CAR group compared to the Co group, which may be related to the health and quality of the animals used in the study. These data corroborate those described in the literature, where CAR reduced the plasmatic and hepatic levels of AOPP, as well as the hepatic levels of MDA and CBO in rats with diabetes induced by a hypercaloric diet and streptozotocin, possibly due to its protective effect against stress oxidative, detoxifying reactive components and producing compounds less harmful to the oxidant system, as is the case of carnosinyl proteins, which inhibit the oxidative conversion of glycated proteins into advanced glycation end-products (AGEs) (Fatih Aydın et al., 2017; Hipkiss et al., 2001). Yılmaz et al., 2017 reported that CAR decreased plasma and hepatic levels of CBO and AOPP in rats with oxidative stress induced by methylglyoxal, associating this activity with its potential antioxidant effect, as an ion chelator and ROS scavenger, preventing modifications in lipids, proteins and nucleic acids caused by metal ions to generate free radicals or by ROS themselves. Studies have described that the imidazole ring present in the structure of CAR has an essential role in inhibiting the formation of reactive

species, in addition to the anti-glycation potential of CAR, preventing the formation of abnormal proteins that can generate AGEs (Boldyrev et al., 2013; Chmielewska et al., 2020).

5. Conclusion

The administration of CAR promoted changes in markers for the MASLD pathophysiology. The supplementation of CAR in MASLD was involved with the attenuation of plasma and hepatic lipid deposition, improvement of plasma HDL cholesterol and attenuation of oxidative damage. It was also observed modulation of the PPAR-α mRNA expressions, a key component in the control of lipid metabolism and oxidative functions in liver tissue. These findings suggest that the PPAR-α transcription factor can be a potential target for the CAR effects in MASLD. More studies are still needed to better elucidate and determine the exact way by means CAR induces PPAR-α modulation. For instance, we conclude that supplementation with CAR is effective for treating lipid metabolism dysfunctions and oxidative stress in MASLD.

Acknowledgments

We also acknowledge technical support by the Unidade de Pesquisa Experimental (UNIPEX) of Botucatu Medical School.

Fundings

National Council for Scientific and Technological Development (CNPq) [Grant number 131679/2021-0].

CRediT authorship contribution stetement

Núbia Alves Grandini: Conceptualization, Data curation, Methodology, Project administration, Writing – original draft. **Mariane Róvero Costa:** Conceptualization, Data curation, Methodology. **Cristina Schmitt Gregolin**: Methodology. **Juliana Silva Siqueira**: Data curation, Methodology. **Taynara Aparecida Vieira**: Methodology. **Artur Junio Togneri Ferron**: Methodology. **Fabiane Valentini Francisqueti-Ferron**: Data curation, Methodology. **Guilherme Ribeiro Romualdo**: Data curation, Methodology. **Ana Lúcia dos Anjos Ferreira**: Methodology. **Giancarlo Aldini**: Conceptualization. **Camila Renata Corrêa**: Data curation, Supervision, Project administration. **Fernando Moreto**: Conceptualization, Data curation, Supervision, Project administration, Writing – original draft.

Conflict of interest: none.

References

Aiello, G., Rescigno, F., Meloni, M., Baron, G., Aldini, G., Carini, M., D'Amato, A., 2022. Oxidative Stress Modulation by Carnosine in Scaffold Free Human Dermis Spheroids Model: A Proteomic Study. Int. J. Mol. Sci. 23, 1468. https://doi.org/10.3390/ijms23031468

Al-Sawalha, N.A., Alshogran, O.Y., Awawdeh, M.S., Almomani, B.A., 2019. The effects of L-Carnosine on development of metabolic syndrome in rats. Life Sci. 237, 116905. https://doi.org/10.1016/j.lfs.2019.116905

Albrecht, T., Schilperoort, M., Zhang, S., Braun, J.D., Qiu, J., Rodriguez, A., Pastene, D.O., Krämer, B.K., Köppel, H., Baelde, H., de Heer, E., Anna Altomare, A., Regazzoni, L., Denisi, A., Aldini, G., van den Born, J., Yard, B.A., Hauske, S.J., 2017. Carnosine Attenuates the Development of both Type 2 Diabetes and Diabetic Nephropathy in BTBR ob/ob Mice. Sci. Rep. 7, 44492. https://doi.org/10.1038/srep44492

Aldini, G., de Courten, B., Regazzoni, L., Gilardoni, E., Ferrario, G., Baron, G., Altomare, A., D'Amato, A., Vistoli, G., Carini, M., 2021. Understanding the antioxidant and carbonyl sequestering activity of carnosine: direct and indirect mechanisms. Free Radic. Res. 55, 321–330. https://doi.org/10.1080/10715762.2020.1856830

Arroyave-ospina, J.C., Wu, Z., Geng, Y., Moshage, H., 2021. Role of Oxidative Stress in the Pathogenesis of Non-Alcoholic Fatty Liver Disease : Implications for Prevention and Therapy. Antioxidants 10, 1–24. https://doi.org/https://doi.org/10.3390/antiox10020174

Aydın, A.F., Bingül, İ., Küçükgergin, C., Doğan-Ekici, I., Doğru Abbasoğlu, S., Uysal, M., 2017. Carnosine decreased oxidation and glycation products in serum and liver of high-fat diet and low-dose streptozotocin-induced diabetic rats. Int. J. Exp. Pathol. 98, 278–288. https://doi.org/10.1111/iep.12252

Barski, O.A., Xie, Z., Baba, S.P., Sithu, S.D., Agarwal, A., Cai, J., Bhatnagar, A., Srivastava, S., 2013. Dietary Carnosine Prevents Early Atherosclerotic Lesion Formation in Apolipoprotein E–Null Mice. Arterioscler. Thromb. Vasc. Biol. 33, 1162–1170. https://doi.org/10.1161/ATVBAHA.112.300572

Bayarsaikhan, G., Bayarsaikhan, D., Lee, J., Lee, B., 2022. Targeting Scavenger

534 Receptors in Inflammatory Disorders and Oxidative Stress. Antioxidants 11, 1–21.
535 https://doi.org/http://dx.doi.org/10.3390/antiox11050936

536 Boldyrev, A.A., Aldini, G., Derave, W., 2013. Physiology and pathophysiology of
537 carnosine. Physiol. Rev. 93, 1803–1845.
538 https://doi.org/10.1152/physrev.00039.2012

539 Buzzetti, E., Pinzani, M., Tsochatzis, E.A., 2016. The multiple-hit pathogenesis of non-
540 alcoholic fatty liver disease (NAFLD). Metabolism 65, 1038–1048.
541 https://doi.org/10.1016/j.metabol.2015.12.012

542 Carneros, D., López-Lluch, G., Bustos, M., 2020. Physiopathology of lifestyle
543 interventions in non-alcoholic fatty liver disease (NAFLD). Nutrients 12, 1–23.
544 https://doi.org/10.3390/nu12113472

545 Chen, P.-J., Tseng, J.-K., Lin, Y.-L., Wu, Y.-H.S., Hsiao, Y.-T., Chen, J.-W., Chen, Y.-C.,
546 2017. Protective Effects of Functional Chicken Liver Hydrolysates against Liver
547 Fibrogenesis: Antioxidation, Anti-inflammation, and Antifibrosis. J. Agric. Food
548 Chem. 65, 4961–4969. https://doi.org/10.1021/acs.jafc.7b01403

549 Chen, Z., Tian, R., She, Z., Cai, J., Li, H., 2020. Role of oxidative stress in the
550 pathogenesis of nonalcoholic fatty liver disease. Free Radic. Biol. Med. 152, 116–
551 141. https://doi.org/https://doi.org/10.1016/j.freeradbiomed.2020.02.025

552 Chmielewska, K., Dzierzbicka, K., Inkielewicz-Stępniak, I., Przybyłowska, M., 2020.
553 Therapeutic Potential of Carnosine and Its Derivatives in the Treatment of Human
554 Diseases. Chem. Res. Toxicol. 33, 1561–1578.
555 https://doi.org/10.1021/acs.chemrestox.0c00010

556 Costa, M.R., Garcia, J.L., Silva, C.C.V. de A., Ferron, A.J.T., Francisqueti-Ferron, F.V.,
557 Hasimoto, F.K., Gregolin, C.S., de Campos, D.H.S., de Andrade, C.R., Ferreira,
558 A.L.D.A., Corrêa, C.R., Moreto, F., 2019. Lycopene modulates pathophysiological
559 processes of non-alcoholic fatty liver disease in obese rats. Antioxidants 8, 1–17.
560 https://doi.org/10.3390/antiox8080276

561 Day, C.P., James, O.F.W., 1998. Steatohepatitis: A tale of two “Hits”? Gastroenterology
562 114, 842–845. https://doi.org/10.1016/S0016-5085(98)70599-2

563 Everaert, I., Van der Stede, T., Stautemas, J., Hanssens, M., van Aanhold, C., Baelde,
564 H., Vanhaecke, L., Derave, W., 2021. Oral anserine supplementation does not
565 attenuate type-2 diabetes or diabetic nephropathy in BTBR ob/ob mice. Amino
566 Acids 53, 1269–1277. https://doi.org/10.1007/s00726-021-03033-4

567 Fatih Aydın, A., Küçükgergin, C., Bingül, İ., Doğan-Ekici, I., Doğru-Abbasoğlu, S., Uysal,
568 M., 2017. Effect of Carnosine on Renal Function, Oxidation and Glycation Products
569 in the Kidneys of High-Fat Diet/Streptozotocin-Induced Diabetic Rats. Exp. Clin.
570 Endocrinol. Diabetes 125, 282–289. https://doi.org/10.1055/s-0043-100117

571 Ferron, A.J.T., Aldini, G., Francisqueti-Ferron, F.V., Silva, C.C.V. de A., Bazan, S.G.Z.,
572 Garcia, J.L., Campos, D.H.S. de, Ghiraldeli, L., Kitawara, K.A.H., Altomare, A.,
573 Correa, C.R., Moreto, F., Ferreira, A.L.A., 2019. Protective Effect of Tomato-
574 Oleoresin Supplementation on Oxidative Injury Recoveries Cardiac Function by
575 Improving β-Adrenergic Response in a Diet-Obesity Induced Model. Antioxidants 8,
576 368. https://doi.org/10.3390/antiox8090368

577 Francisqueti-Ferron, F.V., Silva, J.P. das C., Garcia, J.L., Ferron, A.J.T., Kano, H.T.,
578 Silva, C.C.V. de A., Costa, M.R., Nai, G.A., Moreto, F., Corrêa, C.R., 2022.
579 Preventive Effect of Gamma-Oryzanol on Physiopathological Process Related to
580 Nonalcoholic Fatty Liver Disease in Animals Submitted to High Sugar/Fat Diet.
581 Livers 2, 146–157. https://doi.org/10.3390/livers2030013

582 Francisqueti, F.V., Minatel, I., Ferron, A.J.T., Bazan, S.G.Z., Silva, V. dos S., Garcia,
583 J.L., de Campos, D.H.S., Ferreira, A.L., Moreto, F., Cicogna, A.C., Corrêa, C.R.,
584 2017. Effect of Gamma-Oryzanol as Therapeutic Agent to Prevent Cardiorenal
585 Metabolic Syndrome in Animals Submitted to High Sugar-Fat Diet. Nutrients 9.
586 https://doi.org/10.3390/nu9121299

587 Gabbia, D., Cannella, L., Martin, S. De, 2021. The Role of Oxidative Stress in NAFLD –
588 NASH – HCC Transition — Focus on NADPH Oxidases. Biomedicines 9, 1–14.
589 https://doi.org/https://doi.org/10.3390/biomedicines9060687

590 Garcia, J.L., Francisqueti, F.V., Ferraz, A.P. da C.R., Ferron, A.J.T., Costa, M.R.,
591 Gregolin, C.S., de Campos, D.H., dos Santos, K.C., Minatel, I.O., Corrêa, C.R.,
592 2019. High Sugar-Fat Diet Induces Metabolic-Inflammatory Disorders Independent
593 of Obesity Development. Food Nutr. Sci. 10, 664–677.
594 https://doi.org/10.4236/fns.2019.106049

595 Garcia, J.L., Vileigas, D.F., Gregolin, C.S., Costa, M.R., Francisqueti-Ferron, F.V.,
596 Ferron, A.J.T., De Campos, D.H.S., Moreto, F., Minatel, I.O., Bazan, S.G.Z., Corrêa,
597 C.R., 2022. Rice (Oryza sativa L.) bran preserves cardiac function by modulating
598 pro-inflammatory cytokines and redox state in the myocardium from obese rats. Eur.
599 J. Nutr. 61, 901–913. https://doi.org/10.1007/s00394-021-02691-0

600 Giriş, M., Doğru-Abbasoğlu, S., Kumral, A., Olgaç, V., Koçak-Toker, N., Uysal, M., 2014.

601 Effect of carnosine alone or combined with α-tocopherol on hepatic steatosis and
602 oxidative stress in fructose-induced insulin-resistant rats. J. Physiol. Biochem. 70,
603 385–395. https://doi.org/10.1007/s13105-014-0314-7

604 Hipkiss, A.R., Brownson, C., Carrier, M.J., 2001. Carnosine, the anti-ageing, anti-oxidant
605 dipeptide, may react with protein carbonyl groups. Mech. Ageing Dev. 122, 1431–
606 1445. https://doi.org/10.1016/S0047-6374(01)00272-X

607 Hong, T., Chen, Y., Li, X., Lu, Y., 2021. The Role and Mechanism of Oxidative Stress
608 and Nuclear Receptors in the Development of NAFLD. Oxid Med Cell Longev.
609 https://doi.org/https://doi.org/10.1155/2021/6889533

610 Houjeghani, S., Kheirouri, S., Faraji, E., Jafarabadi, M.A., 2018. L-Carnosine
611 supplementation attenuated fasting glucose, triglycerides, advanced glycation end
612 products, and tumor necrosis factor–α levels in patients with type 2 diabetes: a
613 double-blind placebo-controlled randomized clinical trial. Nutr. Res. 49, 96–106.
614 https://doi.org/10.1016/j.nutres.2017.11.003

615 Jia, Q., Xia, Y., Zhang, Q., Wu, H., Du, H., Liu, L., Wang, C., Shi, H., Guo, X., Liu, X., Li,
616 C., Sun, S., Wang, X., Zhao, H., Song, K., Huang, G., Wu, Y., Cui, N., Niu, K., 2015.
617 Dietary patterns are associated with prevalence of fatty liver disease in adults. Eur.
618 J. Clin. Nutr. 69. https://doi.org/10.1038/ejcn.2014.297

619 Ju, C., Tacke, F., 2016. Hepatic macrophages in homeostasis and liver diseases: from
620 pathogenesis to novel therapeutic strategies. Cell. Mol. Immunol. 13, 316–327.
621 https://doi.org/10.1038/cmi.2015.104

622 Kalaz, E.B., Aydin, A.F., Doğan-Ekici, I., Çoban, J., Doğru-Abbasoğlu, S., Uysal, M.,
623 2016. Protective effects of carnosine alone and together with alpha-tocopherol on
624 lipopolysaccharide (LPS) plus ethanol-induced liver injury. Environ. Toxicol.
625 Pharmacol. 42, 23–29. https://doi.org/10.1016/j.etap.2015.12.018

626 Koo, S.-H., 2013. Nonalcoholic fatty liver disease: molecular mechanisms for the hepatic
627 steatosis. Clin. Mol. Hepatol. 19, 210. https://doi.org/10.3350/cmh.2013.19.3.210

628 Li, H., Zhou, Y., Wang, H., Zhang, Meng, Qiu, P., Zhang, Mengna, Zhang, R., Zhao, Q.,
629 Liu, J., 2020. Crosstalk Between Liver Macrophages and Surrounding Cells in
630 Nonalcoholic Steatohepatitis. Front. Immunol. 11.
631 https://doi.org/10.3389/fimmu.2020.01169

632 Liang, W., Menke, A.L., Driessen, A., Koek, G.H., Lindeman, J.H., Stoop, R., Havekes,
633 L.M., Kleemann, R., van den Hoek, A.M., 2014. Establishment of a General NAFLD

634 Scoring System for Rodent Models and Comparison to Human Liver Pathology.
635 PLoS One 9, e115922. https://doi.org/10.1371/journal.pone.0115922

636 Lim, G.E.H., Tang, A., Han Ng, C., Chin, Y.H., Lim, W.H., Tan, D.J.H., Yong, J.N., Xiao,
637 J., Lee, C.W.-M., Chan, M., Chew, N.W., Tan, E.X.X., Siddiqui, M.S., Huang, D.,
638 Noureddin, M., Sanyal, A.J., Muthiah, M.D., 2021. An Observational Data Meta-
639 analysis on the Differences in Prevalence and Risk Factors Between MAFLD vs
640 NAFLD. Clin. Gastroenterol. Hepatol. https://doi.org/10.1016/j.cgh.2021.11.038

641 MATTHEWS, J.J., ARTIOLI, G.G., TURNER, M.D., SALE, C., 2019. The Physiological
642 Roles of Carnosine and β-Alanine in Exercising Human Skeletal Muscle. Med. Sci.
643 Sport. Exerc. 51, 2098–2108. https://doi.org/10.1249/MSS.0000000000002033

644 Mong, M.C., Chao, C.Y., Yin, M.C., 2011. Histidine and carnosine alleviated hepatic
645 steatosis in mice consumed high saturated fat diet. Eur. J. Pharmacol. 653, 82–88.
646 https://doi.org/10.1016/j.ejphar.2010.12.001

647 Nassir, F., 2022. NAFLD: Mechanisms, Treatments, and Biomarkers. Biomolecules 12.
648 https://doi.org/10.3390/biom12060824

649 Oddy, W., Herbison, C., Jacoby, P., Ambrosini, G., O'Sullivan, T., Ayonrinde, O., Olynyk,
650 J., Black, L., Beilin, L., Mori, T., Hands, B., Adams, L., 2013. The Western dietary
651 pattern is prospectively associated with nonalcoholic fatty liver disease in
652 adolescence. Am J Gastroenterol 108, 778–85. https://doi.org/10.1038/ajg.2013.95

653 Rinella, M.E., Lazarus, J. V., Ratziu, V., Francque, S.M., Sanyal, A.J., Kanwal, F.,
654 Romero, D., Abdelmalek, M.F., Anstee, Q.M., Arab, J.P., Arrese, M., Bataller, R.,
655 Beuers, U., Boursier, J., Bugianesi, E., Byrne, C.D., Castro Narro, G.E., Chowdhury,
656 A., Cortez-Pinto, H., Cryer, D., Cusi, K., El-Kassas, M., Klein, S., Eskridge, W., Fan,
657 J., Gawrieh, S., Guy, C.D., Harrison, S.A., Kim, S.U., Koot, B., Korenjak, M.,
658 Kowdley, K., Lacaille, F., Loomba, R., Mitchell-Thain, R., Morgan, T.R., Powell, E.,
659 Roden, M., Romero-Gómez, M., Silva, M., Singh, S.P., Sookoian, S.C., Spearman,
660 C.W., Tiniakos, D., Valenti, L., Vos, M.B., Wai-Sun Wong, V., Xanthakos, S.,
661 Yilmaz, Y., Younossi, Z., Hobbs, A., Villota-Rivas, M., Newsome, P.N., Ajmeral, V.,
662 Alazawi, W., Alkhatry, M., Alkhouri, N., Allen, A., Allison, M., Alswat, K., Alvares-da-
663 Silva, M.R., Alves-Bezerra, M., Armstrong, M.J., Arufe, D., Aschner, P., Baffy, G.,
664 Bansal, M., Bedossa, P., Belfort, R., Berg, T., Berzigotti, A., Betel, M., Bianco, C.,
665 Brass, C., Brosgart, C.L., Brunt, E.M., Buti, M., Caldwell, S., Carr, R., Casanovas,
666 T., Castera, L., Caussy, C., Cerda, E., Chalasani, N., Chan, W.K.,
667 Charatcharoenwitthaya, P., Charlton, M., Cheung, A., Chiodi, D., Chung, R., Cohen,

668 D., Corey, K., Cotrim, H.P., Crespo, J., Dassanayake, A., Davidson, N., De Knegt,
669 R., De Ledinghen, V., Demir, M., Diaz, S., Diehl, A.M., Dimmig, B., Dirchwolf, M.,
670 Duseja, A., Dvorak, K., Ekstedt, M., El Wakil, R., Ferraz, M.L., Friedman, S., Fuchs,
671 M., Gastaldelli, A., Geerts, A., Geier, A., Girala, M., Goh, G., Goossens, N.,
672 Graupera, I., Hagström, H., Henry, Z., Hunyady, B., Hutchison, A., Isaacs, S.,
673 Jornayvaz, F., Kemp, C., Kile, D., Kim, W., Kleiner, D., Kohli, R., Kugelmas, M.,
674 Lavine, J., Lazo, M., Leite, N., Lozano, A., Luukkonen, P., Macedo, P., Mansour,
675 D., Marchesini, G., Marciano, S., Martinez, K., Mateva, L.V., Mato, J.M., McCary,
676 A., Miele, L., Mikolasevic, I., Miller, V., Moreno, R., Moylan, C., Nakajima, A., Nault,
677 J.C., Norris, S., Noureddin, M., Oliveira, C.P., Ong, A., Padilla, M., Pais, R.,
678 Panduro, A., Panigrahi, M.K., Papatheodoridis, G., Pelusi, S., Pérez, M., Escobar,
679 J.P., Perseghin, G., Pessoa, M., Petta, S., Pinzani, M., Lupsor, M.P., Rabiee, A.,
680 Romeo, S., Rotman, Y., Rowe, I., Salupere, R., Satapathy, S., Schattenberg, J.M.,
681 Schaufert, W., Schnabl, B., Seim, L., Serfaty, L., Shapiro, D., Singal, A.K.,
682 Skladany, L., Stefan, N., Stine, J., Sundaram, S., Svegliati-Baroni, G., Szabo, G.,
683 Tacke, F., Tanwandee, T., Targher, G., Terrault, N., Tetri, B., Thiele, M.,
684 Tisthammer, B., Delgadillo, A.T., Trauner, M., Tsochatzis, E., Van Kleef, L., Van
685 Mil, S., VanWagner, L., Velarde Ruiz Velasco, J.A., Vesterhus, M., Vilar-Gomez,
686 E., Watt, K., Wattacheril, J., Wilkins, F., Willemse, J., Zekry, A., Zelber-Sagi, S.,
687 2023. A multi-society Delphi consensus statement on new fatty liver disease
688 nomenclature. J. Hepatol. https://doi.org/10.1016/j.jhep.2023.06.003

689 Rives, C., Fougerat, A., Ellero-simatos, S., Loiseau, N., Guillou, H., Gamet-Payrastre,
690 L., Wahli, W., 2020. Oxidative Stress in NAFLD : Role of Nutrients and Food
691 Contaminants. Biomolecules 10. https://doi.org/10.3390/biom10121702

692 Romualdo, G.R., Valente, L.C., Sprocatti, A.C., Bacil, G.P., de Souza, I.P., Rodrigues,
693 J., Rodrigues, M.A.M., Vinken, M., Cogliati, B., Barbisan, L.F., 2022. Western diet-
694 induced mouse model of non-alcoholic fatty liver disease associated with metabolic
695 outcomes: Features of gut microbiome–liver–adipose tissue axis. Nutrition 103–
696 104, 111836. https://doi.org/10.1016/j.nut.2022.111836

697 Sabir, U., Irfan, H.M., Alamgeer, Ullah, A., Althobaiti, Y.S., Asim, M.H., 2022. Reduction
698 of Hepatic Steatosis, Oxidative Stress, Inflammation, Ballooning and Insulin
699 Resistance After Therapy with Safranal in NAFLD Animal Model: A New Approach.
700 J. Inflamm. Res. 15, 1293–1316. https://doi.org/10.2147/JIR.S354878

701 Salvoza, N., Giraudi, P.J., Tiribelli, C., Rosso, N., 2022. Natural Compounds for
702 Counteracting Nonalcoholic Fatty Liver Disease (NAFLD): Advantages and

703 Limitations of the Suggested Candidates. Int. J. Mol. Sci. 23.
704 https://doi.org/10.3390/ijms23052764

705 Schnuck, J.K., Sunderland, K.L., Kuennen, M.R., Vaughan, R.A., 2016. Characterization
706 of the metabolic effect of β-alanine on markers of oxidative metabolism and
707 mitochondrial biogenesis in skeletal muscle. J. Exerc. Nutr. Biochem. 20, 34–41.
708 https://doi.org/10.20463/jenb.2016.06.20.2.5

709 Schwank-Xu, C., Forsberg, E., Bentinger, M., Zhao, A., Ansurudeen, I., Dallner, G.,
710 Catrina, S.-B., Brismar, K., Tekle, M., 2021. L-Carnosine Stimulation of Coenzyme
711 Q10 Biosynthesis Promotes Improved Mitochondrial Function and Decreases
712 Hepatic Steatosis in Diabetic Conditions. Antioxidants 10, 793.
713 https://doi.org/10.3390/antiox10050793

714 Siqueira, J.S., Nakandakare-Maia, E.T., Vieira, T.A., Palacio, T.L.N., Grandini, N.A.,
715 Belin, M.A.F., Nai, G.A., Moreto, F., Altomare, A., Baron, G., Aldini, G., Francisqueti-
716 Ferron, F.V., Correa, C.R., 2023. Effect of Bergamot Leaves (Citrus bergamia) in
717 the Crosstalk between Adipose Tissue and Liver of Diet-Induced Obese Rats.
718 Livers 3, 258–270. https://doi.org/10.3390/livers3020017

719 Siqueira, J.S., Vieira, T.A., Nakandakare-Maia, E.T., Palacio, T.L.N., Sarzi, F., Garcia,
720 J.L., de Paula, B.H., Bazan, S.G.Z., Baron, G., Tucci, L., Janda, E., Altomare, A.,
721 Gado, F., Ferron, A.J.T., Aldini, G., Francisqueti-Ferron, F.V., Correa, C.R., 2022.
722 Bergamot leaf extract treats cardiorenal metabolic syndrome and associated
723 pathophysiological factors in rats fed with a high sugar fat diet. Mol. Cell. Endocrinol.
724 556, 111721. https://doi.org/10.1016/j.mce.2022.111721

725 Todisco, S., Santarsiero, A., Convertini, P., De Stefano, G., Gilio, M., Iacobazzi, V.,
726 Infantino, V., 2022. PPAR Alpha as a Metabolic Modulator of the Liver: Role in the
727 Pathogenesis of Nonalcoholic Steatohepatitis (NASH). Biology (Basel). 11, 792.
728 https://doi.org/10.3390/biology11050792

729 Vancells Lujan, P., Viñas Esmel, E., Sacanella Meseguer, E., 2021. Overview of non-
730 alcoholic fatty liver disease (Nafld) and the role of sugary food consumption and
731 other dietary components in its development. Nutrients 13.
732 https://doi.org/10.3390/nu13051442

733 White, U., Ravussin, E., 2019. Dynamics of adipose tissue turnover in human metabolic
734 health and disease. Diabetologia 62, 17–23. https://doi.org/10.1007/s00125-018-
735 4732-x

736 Yang, D.K., Jo, D.G., 2018. Mulberry Fruit Extract Ameliorates Nonalcoholic Fatty Liver
737 Disease (NAFLD) through Inhibition of Mitochondrial Oxidative Stress in Rats.
738 Evidence-based Complement. Altern. Med. 2018.
739 https://doi.org/10.1155/2018/8165716

740 Yılmaz, Z., Kalaz, E.B., Aydın, A.F., Soluk-Tekkeşin, M., Doğru-Abbasoğlu, S., Uysal,
741 M., Koçak-Toker, N., 2017. The effect of carnosine on methylglyoxal-induced
742 oxidative stress in rats. Arch. Physiol. Biochem. 123, 192–198.
743 https://doi.org/10.1080/13813455.2017.1296468

744 Yki-Järvinen, H., Luukkonen, P.K., Hodson, L., Moore, J.B., 2021. Dietary carbohydrates
745 and fats in nonalcoholic fatty liver disease. Nat. Rev. Gastroenterol. Hepatol. 18,
746 770–786. https://doi.org/10.1038/s41575-021-00472-y

747 Younossi, Z.M., Koenig, A.B., Abdelatif, D., Fazel, Y., Henry, L., Wymer, M., 2016. Global
748 epidemiology of nonalcoholic fatty liver disease—Meta-analytic assessment of
749 prevalence, incidence, and outcomes. Hepatology 64, 73–84.
750 https://doi.org/10.1002/hep.28431

751

Effects of carnosine supplementation on markers for the pathophysiological development of metabolic dysfunction-associated steatotic liver disease in a diet-induced model

Núbia Alves Grandini[a*], Mariane Róvero Costa[a], Cristina Schmitt Gregolin[a], Juliana Silva Siqueira[a], Taynara Aparecida Vieira[a], Artur Junio Togneri Ferron[b], Fabiane Valentini Francisqueti-Ferron[b], Guilherme Ribeiro Romualdo[a], Ana Lúcia dos Anjos Ferreira[a], Giancarlo Aldini[c], Camila Renata Corrêa[a], Fernando Moreto[a].

[a] São Paulo State university (UNESP), Medical School, 18618687 Botucatu, Brazil
[b] Integrated Colleges of Bauru (FIB), 17056-100, Brazil
[c] Department of Pharmaceutical Sciences, University of Milan, 20133 Milan, Italy

*Corresponding author

Núbia Alves Grandini, Botucatu Medical School, São Paulo State University (UNESP), Professor Montenegro Avenue, Botucatu, 186186687, Brazil. E-mail address: nubia.grandini@unesp.br

Abstract

Consumption of diets high in sugar and fat is related to the development of Metabolic dysfunction-associated steatotic liver disease (MASLD). Carnosine (CAR) is a dipeptide with antioxidant and anti-inflammatory action and has been studied for treating diseases. This work aimed to evaluate the effects of CAR on diet-induced MASLD in rats. Male Wistar rats were distributed into 2 groups (17 weeks): normocaloric (Co, n=12), and hypercaloric diet rich in lipids and simple carbohydrates (MASLD, n=12). After, the animals were redistributed to begin the treatment with CAR (4 weeks): Co (n=6), Co + CAR (n=6), MASLD (n=6), and MASLD + CAR (n=6), administered intraperitoneally (250mg/kg). Evaluations included nutritional, hormonal and metabolic parameters; hepatic steatosis, inflammatory and oxidative markers. MASLD group had a higher adiposity index, systolic blood pressure, glucose, plasma and liver triglycerides and cholesterol, insulin, hepatic steatosis, oxidative markers, and lower PPAR-α (Peroxisome Proliferator-activated receptor α), compared to the Co. CAR attenuated plasma and hepatic triglyceride and cholesterol levels, hepatic steatosis, CD68+ macrophages, and hepatic oxidative markers, in addition to increasing HDL cholesterol levels and PPAR-α, compared to the untreated MASLD group. CAR acts in importants pathophysiological processes of MASLD and may be a therapeutic compound to control the disease.

Keywords: Metabolic dysfunction-associated steatotic liver disease, carnosine, obesity, hypercaloric diet.

1. Introduction

Non-alcoholic fatty liver disease (NAFLD) is the most common liver injury, which affects about a third of the world's population and is defined by the accumulation of fat in liver tissue without alcohol consumption and other liver damage (Younossi et al., 2016). In 2023, a new terminology and definition were proposed, starting to be called Metabolic dysfunction-associated steatotic liver disease (MASLD). Therefore, the MASLD is based on hepatic steatosis with one of the five cardiometabolic risk factors: overweight or obesity, type 2 diabetes mellitus or hyperglycemia, hypertension or antihypertensive drug treatment, and dyslipidemia (Rinella et al., 2023).

MASLD has a spectrum of evolution from simple steatosis and can involve Metabolic disfunction-associated steatohepatitis (MASH) and even liver cancer (Carneros et al., 2020; Francisqueti-Ferron et al., 2022; Rinella et al., 2023). According to a survey based on data from Europe, North America, and Asia, the prevalence of patients with MASLD is around 39% (Lim et al., 2021), while MASH affects around 5% of the world's population (Younossi et al., 2016). Its pathogenesis is still not well defined, but there are two theories for its development: the first is the "two hits" theory, where it is believed that the first aggression is the imbalance caused by insulin resistance (IR) between the hepatic pathways of acquisition and elimination of lipids, and the second attack involves the processes of inflammation and oxidation (Day and James, 1998). The second theory is that its development takes place from a "multiple hits" model, where several aggressive agents trigger this injury, being genetic, epigenetic, nutritional, and inflammatory, including changes in the microbiota, IR, and oxidative stress (Buzzetti et al., 2016; Day and James, 1998).

The Western diet, rich in simple carbohydrates and fats, is a crucial precursor factor of MASLD, which can cause harmful effects on the liver by accumulating these macronutrients (Rives et al., 2020; Vancells Lujan et al., 2021). Data in the literature indicate that women who consume a diet high in sugar and fat have a 119% greater risk (OR, 2.19; 95% CI, 1.40–3.46) of developing fatty liver disease (Jia et al., 2015); similar data were found for adolescents aged 17 years who had the same Western diet consumption pattern (Oddy et al., 2013). The accumulation of fatty acids in the liver generates hepatic steatosis. It favors the excessive production of ROS (reactive oxygen species), causing an imbalance in the antioxidant system and, consequently, oxidative

stress, which can cause various cellular damage (Arroyave-ospina et al., 2021; Yki-Järvinen et al., 2021).

Given the complexity of MASLD and its consequences, the search for forms of prevention and treatment is necessary. Currently, there is no specific pharmacological treatment for this disease, only drugs that treat specific metabolic alterations, such as dyslipidemia and hyperglycemia, are used (Nassir, 2022; Salvoza et al., 2022). On the other hand, the search for bioactive compounds that can be used to improve these conditions emerges, and one of these compounds is carnosine (CAR), a natural dipeptide composed of β-alanine and L-histidine, which can be found in the human body, in higher concentrations in skeletal muscle and brain (Aldini et al., 2021).

For many years CAR was the focus of studies only related to improving the performance of physical exercises, mainly due to its buffering capacity in the muscles (Matthews et al., 2019). However, CAR has been identified as a potential therapeutic agent in treating diseases due to its antioxidant, anti-inflammatory, and ROS-sequestering activity (Chmielewska et al., 2020). Some studies demonstrated that CAR was able to attenuate the development of type 2 diabetes in ob/ob mice (Albrecht et al., 2017), improve parameters related to metabolic syndrome induced by diet in Wistar rats (Al-Sawalha et al., 2019), as well as improve hepatic steatosis in mice that consumed a high-fat diet (Mong et al., 2011) and in a model of type 2 diabetes in db/db mice (Schwank-Xu et al., 2021). Faced with the need to clarify the biological effects of CAR and the scarcity of studies relating this dipeptide to MASLD, the present study aimed to verify the effects of CAR supplementation on markers of the MASLD pathophysiology induced by diet in rats.

2. Material and Methods

2.1. Animals and Experimental Protocol

This study was approved by the Ethics Committee on Animal Use (nº 1322/2019). It was carried out following the Guide for the Care and Use of Laboratory Animals published by the U.S. National Institutes of Health. Male Wistar rats from the Central Animal Facility of the Faculty of Medicine of Botucatu, approximately 21 days old, were kept in individual cages in an environment with temperature (24±2ºC), humidity (55±5%) and light (light cycle-dark 12h) controlled. Initially, they were distributed into two experimental groups, fed different diets for MASLD induction: normocaloric (n=12) and hypercaloric rich in sugar and fat (n=12). On the 17th week, after the difference between plasma triglycerides, defined as an inclusion criterion, the animals were redistributed into

four groups for treatment: a control group that continued receiving the normocaloric diet (co, n=6), a control group that received the normocaloric diet treated with carnosine (Co+CAR, n=6), a group that continued receiving the hypercaloric diet (MASLD, n=6) and a group that received the hypercaloric diet treated with carnosine (MASLD+CAR, n= 6), for four weeks. Feed and water were offered ad libitum. The animals that received the hypercaloric diet also received sucrose in their drinking water at a concentration of 25% throughout the experiment. Both diets were produced according Francisqueti et al. (2017), and are described in Table 1. The groups received CAR supplementation (250 mg/kg/day) or vehicle (sterile saline solution, 0.9% NaCl) intraperitoneally for four weeks. At the end of the 21 weeks, the animals fasted for 8 hours and then were anesthetized (Thiopental 120 mg/kg/i.p.) and euthanized by decapitation. Blood samples, adipose tissue, and liver were collected.

Table 1. Diet composition and nutritional values.

Components	Normocaloric	Hypercaloric
Soybean meal (g/kg)	335	340
Sorghum (g/kg)	278	80
Soy hulls (g/kg)	188,5	116,7
Dextrin (g/kg)	146,5	20
Maize starch (g/kg)	278	80
Sucrose (g/kg)	-	80
Fructose (g/kg)	-	180
Soybean oil (g/kg)	23	-
Lard (g/kg)	-	154,3
Minerals (g/kg)	25	25
Salt (g/kg)	4	4

2.2. Carnosine Supplementation

CAR (L-carnosine) was administered intraperitoneally (250 mg/kg) for four weeks after induction. The dose was defined based on studies where CAR presented effective results and did not generate toxic and/or adverse effects on the animals (Aydın et al., 2017; Kalaz et al., 2016). The infusion was performed using a 30G needle, with a liquid volume close to 500 µL being injected. The product CarnoPureTM (Flamma S.p.A., Chignolo d'Isola, Bergamo, Italy) was used exclusively for scientific experiments and used in studies abroad. This product was kindly provided by this company, free of charge, for carrying out this experiment.

2.3. Nutritional characterization and obesity

Nutritional characterization was evaluated based on feed, water, and caloric intake (feed and water). Food and water intake were calculated daily from the individual leftovers of each animal. Caloric intake was calculated through food intake multiplied by the energy value of each diet. The characterization of obesity was based on weight gain and adiposity index. Weight gain was calculated by the difference between the final weight and the initial weight of the animals [weight gain (g)=final weight (g) - initial weight (g)]. The adiposity index represents the ratio between the sum of fat deposits (visceral, epididymal, and retroperitoneal) and the final weight of the animals (adiposity index = sum of fat deposits (g)/final weight (g) x 100) (Costa et al., 2019).

2.4. Systolic Blood Pressure

Systolic blood pressure (SBP) was measured by the indirect method of tail plethysmography using an electric sphygmomanometer Narco Bio-System® PE 300, model 709-0610 (International Biomedical, Inc, Houston, Texas, USA). For this purpose, the animals were kept for 5 minutes in a wooden box heated between 38ºC and 40ºC to stimulate arterial vasodilation. Afterward, the cuff was attached to the tail of each animal and inflated (200 mmHg), and deflated, allowing the recording of arterial pulses collected in a Gould RS 3200 polygraph (Gould Instrumenta Valley View, Ohio, USA). The mean of the three PAS readings was recorded for each animal (Siqueira et al., 2022).

2.5. Biochemical and Hormonal Analysis

Glucose was determined using a glucometer (Accu-Check Performa; Roche Diagnostics, Indianapolis, IN, USA). The concentrations of urea, creatinine, uric acid, triglycerides, total cholesterol and its fractions, HDL cholesterol and non-HDL cholesterol (n-HDL) were analyzed by the enzymatic colorimetric method with commercial kits (BioClin®, Belo Horizonte, MG, Brazil) in automated biochemical equipment (Chemistry Analyzer BS-200, Mindray Medical International Limited, Shenzhen, China).

The insulin level was measured using the indirect enzyme immunoassay (ELISA) method using commercial kits (Linco Research Inc., R&D Systems, Millipore, and B-Bridge International Inc.), and the reading was performed on a Spectramax 190 microplate spectrophotometer (Molecular Devices®, Sunnyvale, CA, USA). The IR assessment was performed using the Homeostasis Model Index - Insulin Resistance (HOMA-IR) using glycemia and plasma insulin parameters. The calculation of the HOMA index obeyed the following formula: insulin (µl U/mL) x blood glucose (mmol/L) / 22.5 (Francisqueti-Ferron et al., 2022).

2.6. Liver Tissue Analysis

2.6.1. Histological Parameters

After collection, liver tissue was stored in 4% paraformaldehyde with 0.1M phosphate buffer (pH=7.4) during the first 24 hours. Afterward, the tissue was transferred

to ethyl alcohol, and the samples were embedded in paraffin to obtain five µm-thick sections. Such sections (one per animal) were stained with Hematoxylin & Eosin (HE) and evaluated for steatosis, taking into account the macro and microvesicular aspects, according to the NAFLD Activity Score (NAS) parameter (Liang et al., 2014). Then, ten fields were randomly selected (20x objective), which were evaluated in each section, and the following scores were considered: 0 (<5% of the microscopic field), 1 (5-33%), 2 (33-66%), or 3 (>66%). Other liver samples were frozen and included in an Optimal Cutting Temperature medium (Tissue-Trek, USA), and 10 µm sections were obtained and stained with Oil red (Sigma Aldrich, USA) to obtain representative photos. To assess the presence and deposition of collagen sections samples were stained with picrosirius red with subsequent detection by refringent images on optical microscope. The METAVIR score system was used to evaluate the level of fibrosis: F0: no fibrosis; F1: portal fibrosis without septa; F2: portal fibrosis with septa; F3: septa without cirrhosis; F4: cirrhosis.

2.6.2. Immunohistochemistry for CD68

Other 5 µm thick liver sections were submitted to antigen retrieval in 0.01M citrate buffer (pH 6.0, 120ºC, five min.) in a Pascal pressure chamber (Dako Cytomation, Denmark). After blocking endogenous peroxidase with 10% H2O2 in phosphate-buffered saline (PBS) (15 minutes), the slides were treated with skimmed milk for 60 minutes to block nonspecific binding. Then, the histological sections were incubated in a humid chamber (4ºC overnight) with a primary anti-CD68 antibody solution (macrophages, ab125212, 1:500 dilution, Abcam, UK). Then, the slides were incubated with HRP polymer (Horseradish peroxidase) in a single step (EasyPath - Erviegas, Brazil) (20 minutes at room temperature). The reactions were revealed with the chromogen 3'3-diaminobenzidine (DAB) (Sigma Aldrich, USA), and the slides were counterstained with Harris hematoxylin. CD68+ macrophages were counted in 10 randomly selected fields (20x) and divided by field area (mm²) using Image J software (NIH, USA) (Romualdo et al., 2022).

2.6.3. Oxidative Stress markers

Malondialdehyde (MDA) level was used to assess lipid peroxidation. Briefly, 250 µL of supernatant from hepatic tissue was added to 750 µL of 10% trichloroacetic acid for protein precipitation. The samples were centrifuged (3000 rpm, for 5 minutes; Eppendorf® Centrifuge 5804-R, Hamburg, Germany), and the supernatant was removed. Thiobarbituric acid (ATB) was added at a ratio of 0.67% (1:1), and the samples were heated for 15 minutes at 100°C. After cooling, the reading was performed at 535 nm in the Spectra Max 190 microplate reader (Molecular Devices®, Sunnyvale, CA, USA). The MDA concentration was obtained by the molar extinction coefficient (1.56 x

105 M-1-cm-1) and the absorption of the samples, and the final result was reported in nmol/g of protein (Siqueira et al., 2023).

To quantify protein carbonylation (CBO), 100 µL of liver tissue homogenate was used for 100 µL of 2,4-dinitrophenylhydrazine (DNPH, 10mM in 2M HCl). The samples were incubated for 10 minutes at room temperature, and then 50 µL of sodium hydroxide (6M NaOH) was added and incubated again for 10 minutes at room temperature. Reading at 450 nm was performed on a Spectramax 190 microplate reader (Molecular Devices®, Sunnyvale, CA, USA). The results were obtained by the molar extinction coefficient (22,000 M -1 cm -1) of DNPH and expressed in nmol/g of protein. Protein carbonylation levels were expressed in nmol of DNPH/mg of protein (Garcia et al., 2022).

Advanced oxidation protein products (AOPP) were detected in liver tissue. Tissue samples were homogenized in PBS buffer at 1:10 (sample:PBS). AOPP quantification was performed by diluting 1:5 of 200 µl of the sample (homogenate). 200 µl of Chloramine-T (0-100 umol/L) was used for the calibration curve, and 200 µl of PBS as a blank. 10 µl of 1.16M KI (potassium iodide) and 20 µl of acetic acid were added to the samples. Absorbance was read immediately at 340 nm (Multiskan Ascent spectrophotometer, Labsystems, Vantaa, Finland). The final concentration of AOPP is expressed in chloramin units (umol/L), and the result in the liver tissue is corrected for the amount of protein (Ferron et al., 2019).

2.6.4. Hepatic Levels of Triglycerides and Cholesterol

Intracellular levels of hepatic triglycerides and cholesterol were determined by a colorimetric method (Colorimetric Triglycerides and Cholesterol Assay Kit; Cayman Chemical, Ann Arbor, MI, USA). The results were corrected for the amount of tissue (Francisqueti-Ferron et al., 2022).

2.7. Gene Expressions

Gene expression of peroxisome proliferator-activated receptor α (PPAR-α; gene *Ppara*, primers F-AGATGGGCTGGTTCTTCCTC and R-CAGTGCATTTGCCAGG), very long-chain acyl-CoA dehydrogenase (VLCAD, gene *Acadvl*, primers F-ATGGAATTCATGGCCAGTGAGGCCACTC and R-TTTACGAATTCTCAGACTCTAAGGGGGT) and β-actin (gene *Actb*, primers F-GGGAAATCGTGCGTGACAT and R-CAGGAGGAGCAATGATCTT) were performed using real time PCR (polymerase chain reaction). Total RNA (ribonucleic acid) was extracted from liver tissue using the TRIzol® reagent (Invitrogen, Carlsbad, CA, USA) according to the manufacturer's specifications. The RNA was subjected to reverse transcription for conversion to cDNA (complementary deoxyribonucleic acid) (High-Capacity cDNA Reverse Transcription Kit, Applied Biosystems, CA, USA) using the

provided primers (Exxtend Biotecnologia Ltda, Campinas-SP, Brazil). The real-time PCR kit used the cDNA (TagMan® Gene Expression Assays, Applied Biosystems, Foster City, CA, USA) to evaluate expressions. The β-actin was used to normalize expressions of PPAR-α and VLCAD.

2.8. Statistical Analysis

Results are expressed as mean ± standard deviation. Two-way ANOVA determined differences between groups, and data were subjected to Tukey's post hoc test to compare all groups. Histological parameters are expressed as medians, and Kruskal-Wallis was used with Tukey's post hoc test. Statistical analyzes were performed using Sigma Plot 12.0 software for Windows (Systat Software Inc., San Jose, CA, USA). A p-value <0.05 was considered statistically significant and all performed statistical analyzes were tested to ensure the power to detect differences among groups and the sample size.

3. Results

3.1. Nutritional characterization and obesity

The nutritional characterization and obesity is presented in Table 2. It is possible to observe that the MASLD and MASLD+CAR groups had lower food intake, higher water, caloric intake, and more significant weight gain when compared to the Co and Co+CAR groups, respectively. There was no difference in the initial body weight between groups. The MASLD group had a higher final weight when compared to the Co group. The adiposity index determined the presence of obesity, and it can be seen that the MASLD induction groups (MASLD and MASLD+CAR) had higher adiposity indices when compared to the control groups (Co and Co+CAR, respectively).

Table 2. Nutritional characterization and obesity.

	Groups				Effects		
	Co	**Co+CAR**	**MASLD**	**MASLD+CAR**	**Diet**	**CAR**	**Interactions**
Food intake (g/day)	37.0 ± 2.31	36.3 ± 2.07	25.6 ± 0.904*	25.3 ± 1.72†	<0.001	0.528	0.858
Water intake (ml/day)	53.2 ± 3.79	52.0 ± 7.17	68.0 ± 4.02*	64.9 ± 3.48†	<0.001	0.320	0.564
Caloric intake (kcal/day)	133 ± 8.28	130 ± 7.42	166 ± 7.84*	168 ± 5.44†	<0.001	0.849	0.584
Initial body weight (g)	324 ± 25.0	324 ± 26.8	320 ± 16.4	314 ± 27.1	0.450	0.775	0.753
Final body weight (g)	502 ± 57.2	477 ± 25.8	569 ± 38.0*	530 ± 68.5	0.008	0.133	0.743
Weight gain (g)	145 ± 48.9	137 ± 23.2	250 ± 34.6*	198 ± 48.6†	<0.001	0.085	0.201
Adiposity index (%)	4.15 ± 1.60	3.12 ± 1.11	8.51 ± 1.03*	7.68 ± 2.56†	<0.001	0.19	0.883

Data are presented as mean ± standard deviation. Effects are the comparison by two-way ANOVA with Tukey's post-hoc test, with p<0.05 as statistically significance. Co: control group; Co+CAR: control group treated with carnosine; MASLD: MASLD induction group; MASLD+CAR: MASLD induction group treated with carnosine. * vs Co; † vs Co+CAR.

3.2. Systolic Blood Pressure

Figure 1 shows the Systolic Blood Pressure (SBP) levels. The MASLD group had a higher SBP compared to the Co group.

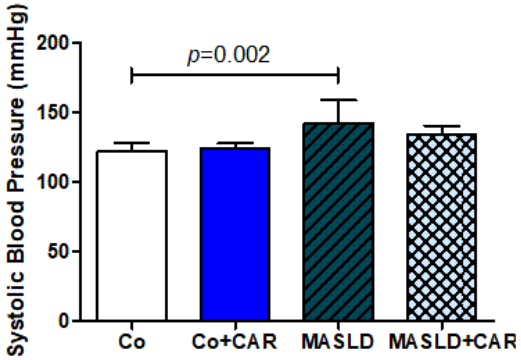

Figure 1. Systolic Blood Pressure Levels. Data are presented as mean ± standard deviation. Comparison by two-way ANOVA with Tukey's post-hoc test. p<0.05 statistically significant. Co: control group; Co+CAR: control group treated with carnosine; MASLD: MASLD induction group; MASLD+CAR: MASLD induction group treated with carnosine.

3.3. Biochemical and hormonal analysis

Table 3 shows the biochemical and hormonal markers. The MASLD and MASLD+CAR groups had lower urea levels when compared to the Co and Co+CAR groups, respectively. There was no significant difference uric acid, and creatinine. ALT levels were significantly lower in control treated with CAR and MASLD induction groups (MASLD and MASLD+CAR) had higher blood glucose levels when compared to the control groups (Co and Co+CAR, respectively). Co+CAR showed lower concentrations of total cholesterol compared to the Co group, while MASLD+CAR showed higher concentrations of total cholesterol compared to the Co+CAR group. Regarding triglycerides, the MASLD and Co+CAR groups had higher and lower concentrations when compared to the Co group. In contrast, the MASLD+CAR group had lower and higher levels when compared to the MASLD and Co+CAR groups, respectively. In addition, the MASLD+CAR group had higher HDL cholesterol (high-density lipoprotein) levels than the MASLD group. There was no statistical difference for non-HDL cholesterol levels. The MASLD and MASLD+CAR groups had higher insulin and HOMA-IR values when compared to the Co and Co+CAR groups, respectively.

Table 3. Biochemical and hormonal markers.

	Groups				Effects		
	Co	**Co+CAR**	**MASLD**	**MASLD+CAR**	**Diet**	**CAR**	**Interactions**
AST (U/l)	155 ± 34.3	125 ± 18.6	114 ± 21.0	130 ± 32.4	0.128	0.532	0.058
ALT (U/l)	104 ± 14.4	69.5 ± 16.1*	83.0 ± 26.5	87.5 ± 21.5	0.858	0.084	0.028
Uric acid (mg/dl)	0.967 ± 0.175	0.800 ± 0.420	1.27 ± 0.761	1.67 ± 1.69	0.150	0.768	0.476

Urea (mg/dl)	58.8 ± 8.66	61.0 ± 9.63	35.0 ± 15.5*	44.2 ± 4.58†	<0.001	0.195	0.417
Creatinine (mg/dl)	4.48 ± 3.08	4.59 ± 5.01	4.48 ± 1.68	4.36 ± 0.985	0.931	0.998	0.930
Blood Glucose (mg/dl)	78.0 ± 8.29	86.3 ± 11.4	88.8 ± 6.74*	97.3 ± 4.50†	0.004	0.020	0.980
Total Cholesterol (mg/dl)	62.3 ± 7.12	46.5 ± 10.1*	52.7 ± 9.63	62.0 ± 8.32†	0.430	0.380	0.002
Triglycerides (mg/dl)	70.4 ± 16.9	41.0 ± 8.32*	205 ± 34.6*	112 ± 27.4#†	<0.001	<0.001	0.004
HDL (mg/dl)	14.5 ± 3.02	14.0 ± 1.79	11.4 ± 2.33	15.5 ± 3.27#	0.471	0.114	0.047
n-HDL (mg/dl)	47.8 ± 4.67	40.5 ± 10.9	40.2 ± 6.59	46.5 ± 5.79	0.785	0.870	0.035
Insulin (ng/ml)	0.224 ± 0.031	0.175 ± 0.039	0.306 ± 0.039*	0.293 ± 0.073†	<0.001	0.132	0.379
HOMA - IR	1.24 ± 0.199	1.07 ± 0.227	1.93 ± 0.304*	2.03 ± 0.535†	<0.001	0.800	0.342

Data are presented as mean ± standard deviation. Effects are the comparison by two-way ANOVA with Tukey's post-hoc test, with $p<0.05$ as statistically significance. Co: control group; Co+CAR: control group treated with carnosine; MASLD: MASLD induction group; MASLD+CAR: MASLD induction group treated with carnosine; AST: aspartate aminotransferase; ALT: alanine aminotransferase; HDL: high density lipoprotein; n-HDL: non-high-density lipoprotein; HOMA-IR: homeostasis model assessment – insulin resistance. * vs Co; # vs MASLD; † vs Co+CAR.

3.4. Liver Tissue Analysis

3.4.1. Histological Parameters

Figure 2 shows the determination of hepatic steatosis by histological parameters. The MASLD induction group supplemented with carnosine (MASLD+CAR) attenuated the steatosis with macro and microvesicular aspects developed by the untreated MASLD induction group (MASLD). Also, picrosirius red staining demonstrate septal fibrosis deposition (black arrow) in MASLD that is significantly reduced in MASLD treated with CAR.

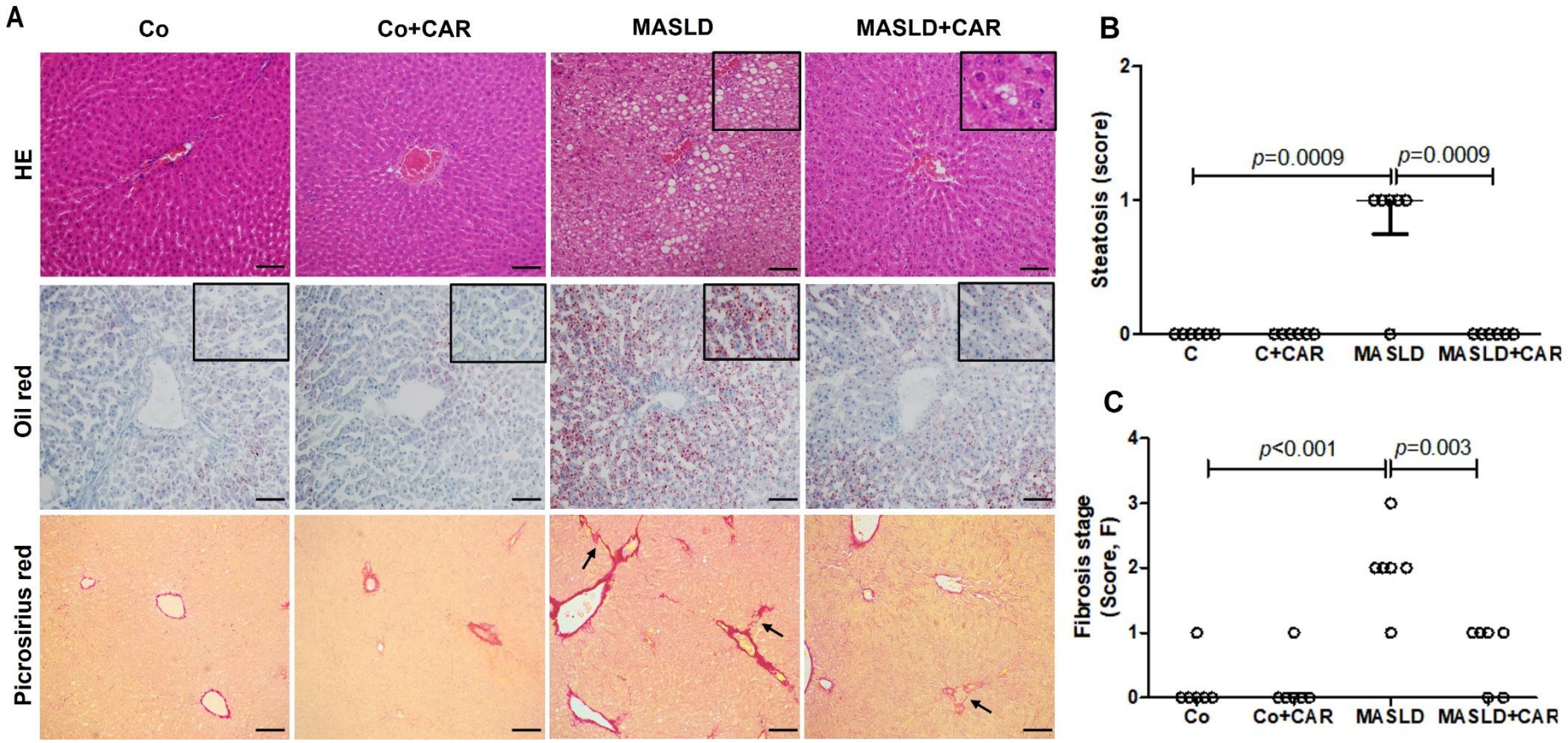

Figure 2. Determination of hepatic steatosis by histological parameters. A) Representative photomicrographs of liver sections stained with HE, Oil red and Picrosirius red (scale bar: 50 µm); B) Steatosis Score; C) Fibrosis Stage. Data are presented as median (max – min) and individual data points, and were analyzed by Kruskal-Wallis with Tukey's post-hoc test. $p<0.05$ statistically significant; n=6 animals/group. Co: control group; Co+CAR: control group treated with carnosine; MASLD: MASLD induction group; MASLD+CAR: MASLD induction group treated with carnosine.

3.4.2. Immunohistochemistry for CD68+

Figure 3 shows the effects of CAR supplementation on the density of CD68+ macrophages. The density of macrophages is lower in the MASLD+CAR group compared to the MASLD group, pointing to an attenuation of the inflammation generated by CAR.

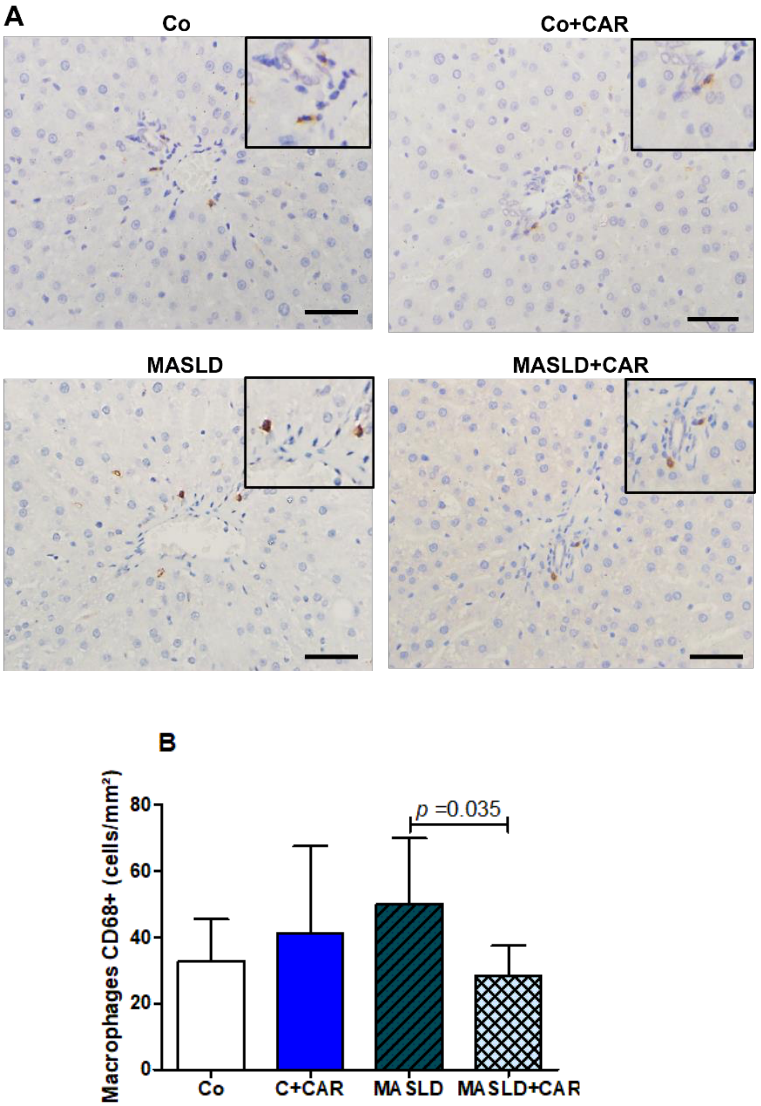

Figure 3. Effects of CAR treatment on CD68+ expression density. A) Representative photomicrographs of immunostained liver sections (details, scale bar: 100 µm). B) Semi-quantitative analysis. Data are presented as mean ± standard deviation and were analyzed by two-way ANOVA with Tukey's post-hoc test. p<0.05 statistically significant; n=6 animals/group. Co: control group; Co+CAR: control group treated with carnosine; MASLD: MASLD induction group; MASLD+CAR: MASLD induction group treated with carnosine.

3.4.3. Oxidative Stress Markers

Figure 4 shows levels of MDA (Figure 4A), CBO (Figure 4B) and AOPP (Figure 4C) in liver tissue. The MASLD group showed higher levels of MDA, CBO, and AOPP compared to the Co group, and in contrast, the MASLD+CAR group attenuated MDA,

CBO, and AOPP levels compared to the MASLD group. Levels of CBO and AOPP of the MASLD+CAR group are elevated compared to the Co+CAR group.

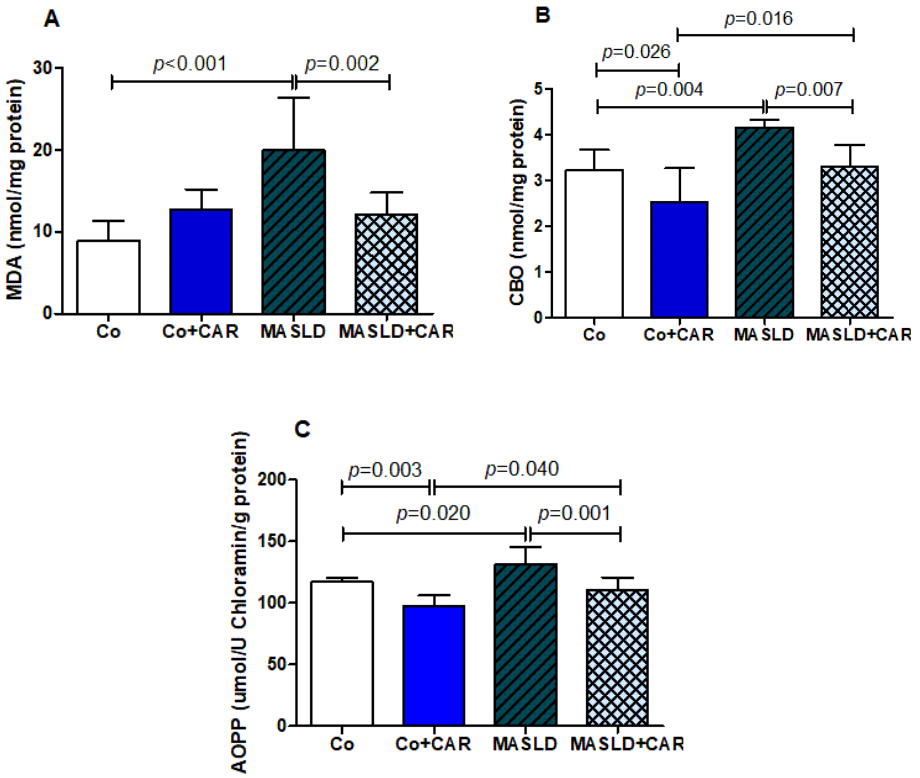

Figure 4. Oxidative Stress Markers. A) Liver levels of MDA; B) Liver levels of CBO; C) Liver levels of AOPP. Data are presented as mean ± standard deviation. Comparison by two-way ANOVA with Tukey's post-hoc test. p<0.05 statistically significant. Co: control group; Co+CAR: control group treated with carnosine; MASLD: MASLD induction group; MASLD+CAR: MASLD induction group treated with carnosine; MDA: Malondialdehyde; CBO: Protein carbonylation; AOPP: Advanced protein oxidation products.

3.4.4. Liver levels of triglycerides and cholesterol

Figure 5 shows the hepatic levels of triglycerides and cholesterol. The MASLD group had higher triglyceride and cholesterol concentrations in the liver than the Co group. The CAR-treated MASLD induction group (MASLD+CAR) had elevated triglyceride concentrations relative to the Co+CAR group but attenuated hepatic triglyceride and cholesterol levels compared to the untreated MASLD induction group.

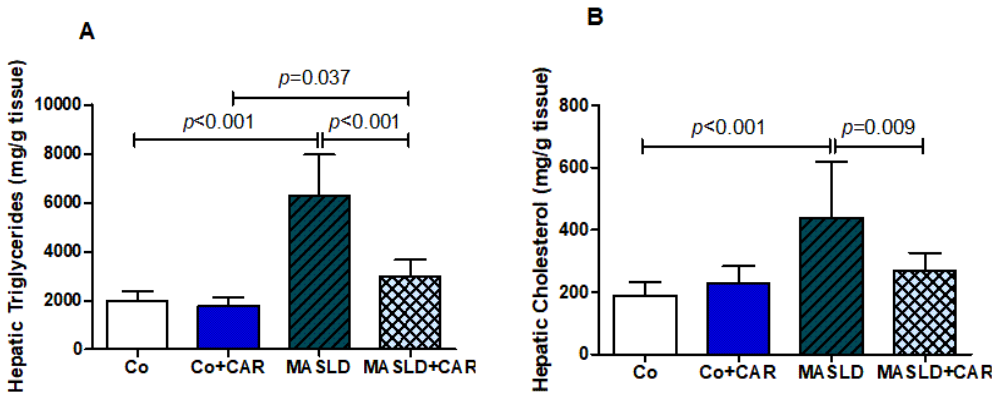

Figure 5. Liver levels of triglycerides and cholesterol. A) Hepatic levels of triglycerides; B) Hepatic cholesterol levels. Data are presented as mean ± standard deviation. Comparison by two-way ANOVA with Tukey's post-hoc test. p<0.05 statistically significant. Co: control group; Co+CAR: control group treated with carnosine; MASLD: MASLD induction group; MASLD+CAR: MASLD induction group treated with carnosine.

3.5. PPAR-α and VLCAD Gene Expressions

Figure 6 shows gene expression by real-time PCR in liver tissue. It can be seen that the MASLD group had lower PPAR-α and VLCAD mRNA levels compared to the Co group. In contrast, the MASLD+CAR group had higher levels of PPAR-α than MASLD group. MASLD+CAR also showed higher VLCAD mRNA levels than MASLD but not enough to get statistical significance.

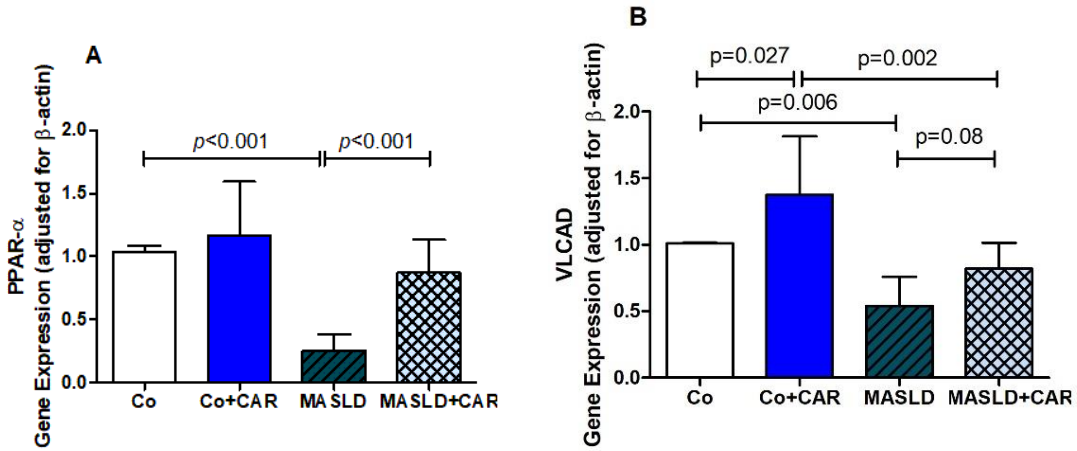

Figura 6. Gene expressions in liver tissue. A) PPAR-α Gene Expression; B) VLCAD Gene Expression. Comparison by two-way ANOVA with Tukey's post-hoc test. p<0.05 statistically significant. Co: control group; Co+CAR: control group treated with carnosine; MASLD: MASLD induction group; MASLD+CAR: MASLD induction group treated with carnosine.

4. Discussion

The present study aimed to verify the effects of CAR supplementation on diet-induced MASLD in rats. Studies have shown that the high consumption of diets rich in

sugars and fats, as well as sugary drinks, favors the development of MASLD, a condition associated with several morbidities, such as metabolic syndrome, insulin resistance, inflammation and oxidative stress (Carneros et al., 2020). In this condition, the present study demonstrated beneficial effects of CAR in the treatment of MASLD by influencing activity of key modulators of lipid metabolism, reflecting in lower lipid deposition and lower inflammatory and oxidative injuries in liver tissue.

MASLD was recently defined by the presence of hepatic steatosis associated with one of the five cardiometabolic risk factors: overweight or obesity, type 2 diabetes mellitus or hyperglycemia, hypertension or antihypertensive drug treatment, and dyslipidemia (Rinella et al., 2023). In this study, the MASLD group presented obesity (higher adiposity index), hypertension, insulin resistance and dyslipidemia, evidencing the presence of the condition. Higher water and caloric intakes were observed in the MASLD group, with a consequent increase in final body weight and weight gain, as observed in other similar studies (Garcia et al., 2022; Siqueira et al., 2022). Although the animals in the MASLD group had lower food intake than the Co group, they had higher sugar-sweetened-water (25% sucrose) consumption, justifying the weight gain and higher final weight of these animals. This dietary habit in association with physical inactivity generates a positive energy balance, which results in hypertrophy and hyperplasia of adipocytes. This change in adipose tissue causes accumulation of fatty acids as well as changes in the production of inflammatory cytokines (Garcia et al., 2019; White and Ravussin, 2019). When hepatocytes reach their lipid-storing capacity, lipotoxicity and hepatocellular stress lead to apoptosis, and then, chemokines are released to activate resident macrophages, kupffer cells, and circulating monocyte-derived macrophages (Li et al., 2020). Macrophages are essential factors in the progression of MASLD. Their activation and proliferation promote several stimuli for inflammatory perpetuation with consequent progression to MASH (Ju and Tacke, 2016). Oxidative stress is also a critical alteration that favors the development of MASLD since the hepatic accumulation of lipids favors the overproduction of ROS, which at high concentrations leads to a decrease in the activity of antioxidant systems, causing several structural and oxidative changes in the metabolism of cellular macromolecules (Bayarsaikhan et al., 2022; Gabbia et al., 2021; Hong et al., 2021). Hepatic storage of triglycerides and cholesterol is an initial mechanism to prevent toxicity; however, excess steatosis can induce lipotoxicity and glucotoxicity in the liver, producing ROS in various organelles (Sabir et al., 2022; Yang and Jo, 2018). Once stablished the pathophysiology of MASLD, the present study aimed to verify the effects of CAR treatment on markers for the development of this condition.

The treatment with CAR did not influence food, water and caloric intake, weight gain, and final weight of the animals in the treated MASLD induction group (MASLD+CAR), corroborating data found in the literature, where CAR supplementation did not influence food and water intake, as well as animal weight parameters (Everaert et al., 2021; Giriş et al., 2014). Treatment with CAR did not influence levels of adiposity index, hypertension, and total cholesterol in the MASLD group. Instead, it was observed attenuated plasma triglyceride levels, as well as improved HDL cholesterol concentrations. Al-Sawalha et al. (2019) conducted a study in rats with metabolic syndrome and CAR supplementation for 16 weeks, where changes similar to those found in our work on the lipid profile were also observed. The positive effects of CAR on lipid parameters were also observed in humans with type 2 diabetes (Houjeghani et al., 2018) who received CAR for 12 weeks, demonstrating that CAR can act as an anti-dyslipidemic agent and may have protective effects in models of obesity-related complications.

The mechanism by which CAR intervenes on lipid profile is not well understood. In the present work, along with a better plasma lipid profile and lower deposition of lipids in liver tissue it was observed important modulatory activity on PPAR-α gene expression. PPAR-α is a key transcription factor that regulates transcription of genes involved in fatty acid β-oxidation and thermogenesis (Todisco et al., 2022). Moreover, in response of PPAR-α activation or not, it was observed a modulatory effect on mRNA expression of VLCAD, an enzyme responsible for the catalysis of the first reaction of the mitochondrial very long chain fatty acids β-oxidation (Koo, 2013). The oxidation of fatty acids, mainly regulated by PPAR-α, reduces the levels of fatty acids available in the liver, using them as an energy source. However, in the face of mitochondrial dysfunction, the β-oxidation process is impaired, thus generating fat accumulation, as well as the production of ROS (Arroyave-ospina et al., 2021; Chen et al., 2020; Mong et al., 2011). In the present study, the MASLD group showed lower PPAR-α gene expression than the Co group. CAR supplementation in the MASLD+CAR increased mRNA levels compared to the MASLD group, pointing to a possible role on this component. Additionally, mRNA levels of VLCAD showed similar behavior, demonstrating high response in Co+CAR and a restoring effect in the MASLD+CAR, even still not statistically significant. There are no data in the literature reporting the role of CAR on PPAR-α, but there are studies where β-alanine, a precursor of CAR, was able to stimulate the expression of PPAR-β/δ, a key regulator of muscle lipid balance, suggesting that histidyl dipeptides can be natural ligands of PPARs (Schnuck et al., 2016). In line with this, these findings suggest a possible role of CAR on dysfunctions of lipid metabolism, in view of the reduction of

plasma and hepatic triglycerides, hepatic cholesterol, steatosis and oxidative stress, as well as an increase in PPAR-α gene expression in MASLD.

Although no significant difference was observed between the MASLD group and the Co group for CD68 expression, CAR significantly attenuated their activation compared to the MASLD group. The reduction of macrophage infiltration in MASLD+CAR is in line with the reduction of collagen deposition marked by Sirius red staining and fibrosis score in the same group, suggesting a possible role of CAR in the atenuation of MASLD progression to MASH. Similar data were found in the literature, where CAR attenuated inflammatory infiltrates (monocytes and macrophages) (Chen et al., 2017). Another study reported a significant decrease in CD68 macrophages in mice with atherosclerotic lesions treated with CAR (Barski et al., 2013). CAR's action on macrophages may be related to its potential to reduce oxidative stress, which is directly related to inflammation. However, CAR may also be acting on MIF, generating a decrease in the activity of CD68 macrophages in the obesity model. Aiello et al., 2022 observed that CAR increased MIF in a 3D skin model, associating this effect with the antioxidant action of CAR and its power to reduce oxidative stress and its positive effect on aging.

In line with this hypothesis, the present work showed that the MASLD group had higher hepatic levels of MDA, carbonyl proteins (CBO), and AOPP in comparison to the control group, but, the treatment with CAR (MASLD+CAR group) attenuated the hepatic concentrations of MDA, CBO, and AOPP in comparison to the MASLD group. It is also possible to notice lower concentrations of CBO and AOPP in the Co+CAR group compared to the Co group, which may be related to the health and quality of the animals used in the study. These data corroborate those described in the literature, where CAR reduced the plasmatic and hepatic levels of AOPP, as well as the hepatic levels of MDA and CBO in rats with diabetes induced by a hypercaloric diet and streptozotocin, possibly due to its protective effect against stress oxidative, detoxifying reactive components and producing compounds less harmful to the oxidant system, as is the case of carnosinyl proteins, which inhibit the oxidative conversion of glycated proteins into advanced glycation end-products (AGEs) (Fatih Aydın et al., 2017; Hipkiss et al., 2001). Yılmaz et al., 2017 reported that CAR decreased plasma and hepatic levels of CBO and AOPP in rats with oxidative stress induced by methylglyoxal, associating this activity with its potential antioxidant effect, as an ion chelator and ROS scavenger, preventing modifications in lipids, proteins and nucleic acids caused by metal ions to generate free radicals or by ROS themselves. Studies have described that the imidazole ring present in the structure of CAR has an essential role in inhibiting the formation of reactive

species, in addition to the anti-glycation potential of CAR, preventing the formation of abnormal proteins that can generate AGEs (Boldyrev et al., 2013; Chmielewska et al., 2020).

5. Conclusion

The administration of CAR promoted changes in markers for the MASLD pathophysiology. The supplementation of CAR in MASLD was involved with the attenuation of plasma and hepatic lipid deposition, improvement of plasma HDL cholesterol and attenuation of oxidative damage. It was also observed modulation of the PPAR-α mRNA expressions, a key component in the control of lipid metabolism and oxidative functions in liver tissue. These findings suggest that the PPAR-α transcription factor can be a potential target for the CAR effects in MASLD. More studies are still needed to better elucidate and determine the exact way by means CAR induces PPAR-α modulation. For instance, we conclude that supplementation with CAR is effective for treating lipid metabolism dysfunctions and oxidative stress in MASLD.

Acknowledgments

We also acknowledge technical support by the Unidade de Pesquisa Experimental (UNIPEX) of Botucatu Medical School.

Fundings

National Council for Scientific and Technological Development (CNPq) [Grant number 131679/2021-0].

CRediT authorship contribution stetement

Núbia Alves Grandini: Conceptualization, Data curation, Methodology, Project administration, Writing – original draft. **Mariane Róvero Costa:** Conceptualization, Data curation, Methodology. **Cristina Schmitt Gregolin**: Methodology. **Juliana Silva Siqueira**: Data curation, Methodology. **Taynara Aparecida Vieira**: Methodology. **Artur Junio Togneri Ferron**: Methodology. **Fabiane Valentini Francisqueti-Ferron**: Data curation, Methodology. **Guilherme Ribeiro Romualdo**: Data curation, Methodology. **Ana Lúcia dos Anjos Ferreira**: Methodology. **Giancarlo Aldini**: Conceptualization. **Camila Renata Corrêa**: Data curation, Supervision, Project administration. **Fernando Moreto**: Conceptualization, Data curation, Supervision, Project administration, Writing – original draft.

Conflict of interest: none.

References

Aiello, G., Rescigno, F., Meloni, M., Baron, G., Aldini, G., Carini, M., D'Amato, A., 2022. Oxidative Stress Modulation by Carnosine in Scaffold Free Human Dermis Spheroids Model: A Proteomic Study. Int. J. Mol. Sci. 23, 1468. https://doi.org/10.3390/ijms23031468

Al-Sawalha, N.A., Alshogran, O.Y., Awawdeh, M.S., Almomani, B.A., 2019. The effects of L-Carnosine on development of metabolic syndrome in rats. Life Sci. 237, 116905. https://doi.org/10.1016/j.lfs.2019.116905

Albrecht, T., Schilperoort, M., Zhang, S., Braun, J.D., Qiu, J., Rodriguez, A., Pastene, D.O., Krämer, B.K., Köppel, H., Baelde, H., de Heer, E., Anna Altomare, A., Regazzoni, L., Denisi, A., Aldini, G., van den Born, J., Yard, B.A., Hauske, S.J., 2017. Carnosine Attenuates the Development of both Type 2 Diabetes and Diabetic Nephropathy in BTBR ob/ob Mice. Sci. Rep. 7, 44492. https://doi.org/10.1038/srep44492

Aldini, G., de Courten, B., Regazzoni, L., Gilardoni, E., Ferrario, G., Baron, G., Altomare, A., D'Amato, A., Vistoli, G., Carini, M., 2021. Understanding the antioxidant and carbonyl sequestering activity of carnosine: direct and indirect mechanisms. Free Radic. Res. 55, 321–330. https://doi.org/10.1080/10715762.2020.1856830

Arroyave-ospina, J.C., Wu, Z., Geng, Y., Moshage, H., 2021. Role of Oxidative Stress in the Pathogenesis of Non-Alcoholic Fatty Liver Disease : Implications for Prevention and Therapy. Antioxidants 10, 1–24. https://doi.org/https://doi.org/10.3390/antiox10020174

Aydın, A.F., Bingül, İ., Küçükgergin, C., Doğan-Ekici, I., Doğru Abbasoğlu, S., Uysal, M., 2017. Carnosine decreased oxidation and glycation products in serum and liver of high-fat diet and low-dose streptozotocin-induced diabetic rats. Int. J. Exp. Pathol. 98, 278–288. https://doi.org/10.1111/iep.12252

Barski, O.A., Xie, Z., Baba, S.P., Sithu, S.D., Agarwal, A., Cai, J., Bhatnagar, A., Srivastava, S., 2013. Dietary Carnosine Prevents Early Atherosclerotic Lesion Formation in Apolipoprotein E–Null Mice. Arterioscler. Thromb. Vasc. Biol. 33, 1162–1170. https://doi.org/10.1161/ATVBAHA.112.300572

Bayarsaikhan, G., Bayarsaikhan, D., Lee, J., Lee, B., 2022. Targeting Scavenger

Receptors in Inflammatory Disorders and Oxidative Stress. Antioxidants 11, 1–21. https://doi.org/http://dx.doi.org/10.3390/antiox11050936

Boldyrev, A.A., Aldini, G., Derave, W., 2013. Physiology and pathophysiology of carnosine. Physiol. Rev. 93, 1803–1845. https://doi.org/10.1152/physrev.00039.2012

Buzzetti, E., Pinzani, M., Tsochatzis, E.A., 2016. The multiple-hit pathogenesis of non-alcoholic fatty liver disease (NAFLD). Metabolism 65, 1038–1048. https://doi.org/10.1016/j.metabol.2015.12.012

Carneros, D., López-Lluch, G., Bustos, M., 2020. Physiopathology of lifestyle interventions in non-alcoholic fatty liver disease (NAFLD). Nutrients 12, 1–23. https://doi.org/10.3390/nu12113472

Chen, P.-J., Tseng, J.-K., Lin, Y.-L., Wu, Y.-H.S., Hsiao, Y.-T., Chen, J.-W., Chen, Y.-C., 2017. Protective Effects of Functional Chicken Liver Hydrolysates against Liver Fibrogenesis: Antioxidation, Anti-inflammation, and Antifibrosis. J. Agric. Food Chem. 65, 4961–4969. https://doi.org/10.1021/acs.jafc.7b01403

Chen, Z., Tian, R., She, Z., Cai, J., Li, H., 2020. Role of oxidative stress in the pathogenesis of nonalcoholic fatty liver disease. Free Radic. Biol. Med. 152, 116–141. https://doi.org/https://doi.org/10.1016/j.freeradbiomed.2020.02.025

Chmielewska, K., Dzierzbicka, K., Inkielewicz-Stępniak, I., Przybyłowska, M., 2020. Therapeutic Potential of Carnosine and Its Derivatives in the Treatment of Human Diseases. Chem. Res. Toxicol. 33, 1561–1578. https://doi.org/10.1021/acs.chemrestox.0c00010

Costa, M.R., Garcia, J.L., Silva, C.C.V. de A., Ferron, A.J.T., Francisqueti-Ferron, F.V., Hasimoto, F.K., Gregolin, C.S., de Campos, D.H.S., de Andrade, C.R., Ferreira, A.L.D.A., Corrêa, C.R., Moreto, F., 2019. Lycopene modulates pathophysiological processes of non-alcoholic fatty liver disease in obese rats. Antioxidants 8, 1–17. https://doi.org/10.3390/antiox8080276

Day, C.P., James, O.F.W., 1998. Steatohepatitis: A tale of two “Hits”? Gastroenterology 114, 842–845. https://doi.org/10.1016/S0016-5085(98)70599-2

Everaert, I., Van der Stede, T., Stautemas, J., Hanssens, M., van Aanhold, C., Baelde, H., Vanhaecke, L., Derave, W., 2021. Oral anserine supplementation does not attenuate type-2 diabetes or diabetic nephropathy in BTBR ob/ob mice. Amino Acids 53, 1269–1277. https://doi.org/10.1007/s00726-021-03033-4

Fatih Aydın, A., Küçükgergin, C., Bingül, İ., Doğan-Ekici, I., Doğru-Abbasoğlu, S., Uysal, M., 2017. Effect of Carnosine on Renal Function, Oxidation and Glycation Products in the Kidneys of High-Fat Diet/Streptozotocin-Induced Diabetic Rats. Exp. Clin. Endocrinol. Diabetes 125, 282–289. https://doi.org/10.1055/s-0043-100117

Ferron, A.J.T., Aldini, G., Francisqueti-Ferron, F.V., Silva, C.C.V. de A., Bazan, S.G.Z., Garcia, J.L., Campos, D.H.S. de, Ghiraldeli, L., Kitawara, K.A.H., Altomare, A., Correa, C.R., Moreto, F., Ferreira, A.L.A., 2019. Protective Effect of Tomato-Oleoresin Supplementation on Oxidative Injury Recoveries Cardiac Function by Improving β-Adrenergic Response in a Diet-Obesity Induced Model. Antioxidants 8, 368. https://doi.org/10.3390/antiox8090368

Francisqueti-Ferron, F.V., Silva, J.P. das C., Garcia, J.L., Ferron, A.J.T., Kano, H.T., Silva, C.C.V. de A., Costa, M.R., Nai, G.A., Moreto, F., Corrêa, C.R., 2022. Preventive Effect of Gamma-Oryzanol on Physiopathological Process Related to Nonalcoholic Fatty Liver Disease in Animals Submitted to High Sugar/Fat Diet. Livers 2, 146–157. https://doi.org/10.3390/livers2030013

Francisqueti, F.V., Minatel, I., Ferron, A.J.T., Bazan, S.G.Z., Silva, V. dos S., Garcia, J.L., de Campos, D.H.S., Ferreira, A.L., Moreto, F., Cicogna, A.C., Corrêa, C.R., 2017. Effect of Gamma-Oryzanol as Therapeutic Agent to Prevent Cardiorenal Metabolic Syndrome in Animals Submitted to High Sugar-Fat Diet. Nutrients 9. https://doi.org/10.3390/nu9121299

Gabbia, D., Cannella, L., Martin, S. De, 2021. The Role of Oxidative Stress in NAFLD – NASH – HCC Transition — Focus on NADPH Oxidases. Biomedicines 9, 1–14. https://doi.org/https://doi.org/10.3390/biomedicines9060687

Garcia, J.L., Francisqueti, F.V., Ferraz, A.P. da C.R., Ferron, A.J.T., Costa, M.R., Gregolin, C.S., de Campos, D.H., dos Santos, K.C., Minatel, I.O., Corrêa, C.R., 2019. High Sugar-Fat Diet Induces Metabolic-Inflammatory Disorders Independent of Obesity Development. Food Nutr. Sci. 10, 664–677. https://doi.org/10.4236/fns.2019.106049

Garcia, J.L., Vileigas, D.F., Gregolin, C.S., Costa, M.R., Francisqueti-Ferron, F.V., Ferron, A.J.T., De Campos, D.H.S., Moreto, F., Minatel, I.O., Bazan, S.G.Z., Corrêa, C.R., 2022. Rice (Oryza sativa L.) bran preserves cardiac function by modulating pro-inflammatory cytokines and redox state in the myocardium from obese rats. Eur. J. Nutr. 61, 901–913. https://doi.org/10.1007/s00394-021-02691-0

Giriş, M., Doğru-Abbasoğlu, S., Kumral, A., Olgaç, V., Koçak-Toker, N., Uysal, M., 2014.

Effect of carnosine alone or combined with α-tocopherol on hepatic steatosis and oxidative stress in fructose-induced insulin-resistant rats. J. Physiol. Biochem. 70, 385–395. https://doi.org/10.1007/s13105-014-0314-7

Hipkiss, A.R., Brownson, C., Carrier, M.J., 2001. Carnosine, the anti-ageing, anti-oxidant dipeptide, may react with protein carbonyl groups. Mech. Ageing Dev. 122, 1431–1445. https://doi.org/10.1016/S0047-6374(01)00272-X

Hong, T., Chen, Y., Li, X., Lu, Y., 2021. The Role and Mechanism of Oxidative Stress and Nuclear Receptors in the Development of NAFLD. Oxid Med Cell Longev. https://doi.org/https://doi.org/10.1155/2021/6889533

Houjeghani, S., Kheirouri, S., Faraji, E., Jafarabadi, M.A., 2018. L-Carnosine supplementation attenuated fasting glucose, triglycerides, advanced glycation end products, and tumor necrosis factor–α levels in patients with type 2 diabetes: a double-blind placebo-controlled randomized clinical trial. Nutr. Res. 49, 96–106. https://doi.org/10.1016/j.nutres.2017.11.003

Jia, Q., Xia, Y., Zhang, Q., Wu, H., Du, H., Liu, L., Wang, C., Shi, H., Guo, X., Liu, X., Li, C., Sun, S., Wang, X., Zhao, H., Song, K., Huang, G., Wu, Y., Cui, N., Niu, K., 2015. Dietary patterns are associated with prevalence of fatty liver disease in adults. Eur. J. Clin. Nutr. 69. https://doi.org/10.1038/ejcn.2014.297

Ju, C., Tacke, F., 2016. Hepatic macrophages in homeostasis and liver diseases: from pathogenesis to novel therapeutic strategies. Cell. Mol. Immunol. 13, 316–327. https://doi.org/10.1038/cmi.2015.104

Kalaz, E.B., Aydin, A.F., Doğan-Ekici, I., Çoban, J., Doğru-Abbasoğlu, S., Uysal, M., 2016. Protective effects of carnosine alone and together with alpha-tocopherol on lipopolysaccharide (LPS) plus ethanol-induced liver injury. Environ. Toxicol. Pharmacol. 42, 23–29. https://doi.org/10.1016/j.etap.2015.12.018

Koo, S.-H., 2013. Nonalcoholic fatty liver disease: molecular mechanisms for the hepatic steatosis. Clin. Mol. Hepatol. 19, 210. https://doi.org/10.3350/cmh.2013.19.3.210

Li, H., Zhou, Y., Wang, H., Zhang, Meng, Qiu, P., Zhang, Mengna, Zhang, R., Zhao, Q., Liu, J., 2020. Crosstalk Between Liver Macrophages and Surrounding Cells in Nonalcoholic Steatohepatitis. Front. Immunol. 11. https://doi.org/10.3389/fimmu.2020.01169

Liang, W., Menke, A.L., Driessen, A., Koek, G.H., Lindeman, J.H., Stoop, R., Havekes, L.M., Kleemann, R., van den Hoek, A.M., 2014. Establishment of a General NAFLD

Scoring System for Rodent Models and Comparison to Human Liver Pathology. PLoS One 9, e115922. https://doi.org/10.1371/journal.pone.0115922

Lim, G.E.H., Tang, A., Han Ng, C., Chin, Y.H., Lim, W.H., Tan, D.J.H., Yong, J.N., Xiao, J., Lee, C.W.-M., Chan, M., Chew, N.W., Tan, E.X.X., Siddiqui, M.S., Huang, D., Noureddin, M., Sanyal, A.J., Muthiah, M.D., 2021. An Observational Data Meta-analysis on the Differences in Prevalence and Risk Factors Between MAFLD vs NAFLD. Clin. Gastroenterol. Hepatol. https://doi.org/10.1016/j.cgh.2021.11.038

MATTHEWS, J.J., ARTIOLI, G.G., TURNER, M.D., SALE, C., 2019. The Physiological Roles of Carnosine and β-Alanine in Exercising Human Skeletal Muscle. Med. Sci. Sport. Exerc. 51, 2098–2108. https://doi.org/10.1249/MSS.0000000000002033

Mong, M.C., Chao, C.Y., Yin, M.C., 2011. Histidine and carnosine alleviated hepatic steatosis in mice consumed high saturated fat diet. Eur. J. Pharmacol. 653, 82–88. https://doi.org/10.1016/j.ejphar.2010.12.001

Nassir, F., 2022. NAFLD: Mechanisms, Treatments, and Biomarkers. Biomolecules 12. https://doi.org/10.3390/biom12060824

Oddy, W., Herbison, C., Jacoby, P., Ambrosini, G., O'Sullivan, T., Ayonrinde, O., Olynyk, J., Black, L., Beilin, L., Mori, T., Hands, B., Adams, L., 2013. The Western dietary pattern is prospectively associated with nonalcoholic fatty liver disease in adolescence. Am J Gastroenterol 108, 778–85. https://doi.org/10.1038/ajg.2013.95

Rinella, M.E., Lazarus, J. V., Ratziu, V., Francque, S.M., Sanyal, A.J., Kanwal, F., Romero, D., Abdelmalek, M.F., Anstee, Q.M., Arab, J.P., Arrese, M., Bataller, R., Beuers, U., Boursier, J., Bugianesi, E., Byrne, C.D., Castro Narro, G.E., Chowdhury, A., Cortez-Pinto, H., Cryer, D., Cusi, K., El-Kassas, M., Klein, S., Eskridge, W., Fan, J., Gawrieh, S., Guy, C.D., Harrison, S.A., Kim, S.U., Koot, B., Korenjak, M., Kowdley, K., Lacaille, F., Loomba, R., Mitchell-Thain, R., Morgan, T.R., Powell, E., Roden, M., Romero-Gómez, M., Silva, M., Singh, S.P., Sookoian, S.C., Spearman, C.W., Tiniakos, D., Valenti, L., Vos, M.B., Wai-Sun Wong, V., Xanthakos, S., Yilmaz, Y., Younossi, Z., Hobbs, A., Villota-Rivas, M., Newsome, P.N., Ajmeral, V., Alazawi, W., Alkhatry, M., Alkhouri, N., Allen, A., Allison, M., Alswat, K., Alvares-da-Silva, M.R., Alves-Bezerra, M., Armstrong, M.J., Arufe, D., Aschner, P., Baffy, G., Bansal, M., Bedossa, P., Belfort, R., Berg, T., Berzigotti, A., Betel, M., Bianco, C., Brass, C., Brosgart, C.L., Brunt, E.M., Buti, M., Caldwell, S., Carr, R., Casanovas, T., Castera, L., Caussy, C., Cerda, E., Chalasani, N., Chan, W.K., Charatcharoenwitthaya, P., Charlton, M., Cheung, A., Chiodi, D., Chung, R., Cohen,

D., Corey, K., Cotrim, H.P., Crespo, J., Dassanayake, A., Davidson, N., De Knegt, R., De Ledinghen, V., Demir, M., Diaz, S., Diehl, A.M., Dimmig, B., Dirchwolf, M., Duseja, A., Dvorak, K., Ekstedt, M., El Wakil, R., Ferraz, M.L., Friedman, S., Fuchs, M., Gastaldelli, A., Geerts, A., Geier, A., Girala, M., Goh, G., Goossens, N., Graupera, I., Hagström, H., Henry, Z., Hunyady, B., Hutchison, A., Isaacs, S., Jornayvaz, F., Kemp, C., Kile, D., Kim, W., Kleiner, D., Kohli, R., Kugelmas, M., Lavine, J., Lazo, M., Leite, N., Lozano, A., Luukkonen, P., Macedo, P., Mansour, D., Marchesini, G., Marciano, S., Martinez, K., Mateva, L.V., Mato, J.M., McCary, A., Miele, L., Mikolasevic, I., Miller, V., Moreno, R., Moylan, C., Nakajima, A., Nault, J.C., Norris, S., Noureddin, M., Oliveira, C.P., Ong, A., Padilla, M., Pais, R., Panduro, A., Panigrahi, M.K., Papatheodoridis, G., Pelusi, S., Pérez, M., Escobar, J.P., Perseghin, G., Pessoa, M., Petta, S., Pinzani, M., Lupsor, M.P., Rabiee, A., Romeo, S., Rotman, Y., Rowe, I., Salupere, R., Satapathy, S., Schattenberg, J.M., Schaufert, W., Schnabl, B., Seim, L., Serfaty, L., Shapiro, D., Singal, A.K., Skladany, L., Stefan, N., Stine, J., Sundaram, S., Svegliati-Baroni, G., Szabo, G., Tacke, F., Tanwandee, T., Targher, G., Terrault, N., Tetri, B., Thiele, M., Tisthammer, B., Delgadillo, A.T., Trauner, M., Tsochatzis, E., Van Kleef, L., Van Mil, S., VanWagner, L., Velarde Ruiz Velasco, J.A., Vesterhus, M., Vilar-Gomez, E., Watt, K., Wattacheril, J., Wilkins, F., Willemse, J., Zekry, A., Zelber-Sagi, S., 2023. A multi-society Delphi consensus statement on new fatty liver disease nomenclature. J. Hepatol. https://doi.org/10.1016/j.jhep.2023.06.003

Rives, C., Fougerat, A., Ellero-simatos, S., Loiseau, N., Guillou, H., Gamet-Payrastre, L., Wahli, W., 2020. Oxidative Stress in NAFLD : Role of Nutrients and Food Contaminants. Biomolecules 10. https://doi.org/10.3390/biom10121702

Romualdo, G.R., Valente, L.C., Sprocatti, A.C., Bacil, G.P., de Souza, I.P., Rodrigues, J., Rodrigues, M.A.M., Vinken, M., Cogliati, B., Barbisan, L.F., 2022. Western diet-induced mouse model of non-alcoholic fatty liver disease associated with metabolic outcomes: Features of gut microbiome–liver–adipose tissue axis. Nutrition 103–104, 111836. https://doi.org/10.1016/j.nut.2022.111836

Sabir, U., Irfan, H.M., Alamgeer, Ullah, A., Althobaiti, Y.S., Asim, M.H., 2022. Reduction of Hepatic Steatosis, Oxidative Stress, Inflammation, Ballooning and Insulin Resistance After Therapy with Safranal in NAFLD Animal Model: A New Approach. J. Inflamm. Res. 15, 1293–1316. https://doi.org/10.2147/JIR.S354878

Salvoza, N., Giraudi, P.J., Tiribelli, C., Rosso, N., 2022. Natural Compounds for Counteracting Nonalcoholic Fatty Liver Disease (NAFLD): Advantages and

Limitations of the Suggested Candidates. Int. J. Mol. Sci. 23. https://doi.org/10.3390/ijms23052764

Schnuck, J.K., Sunderland, K.L., Kuennen, M.R., Vaughan, R.A., 2016. Characterization of the metabolic effect of β-alanine on markers of oxidative metabolism and mitochondrial biogenesis in skeletal muscle. J. Exerc. Nutr. Biochem. 20, 34–41. https://doi.org/10.20463/jenb.2016.06.20.2.5

Schwank-Xu, C., Forsberg, E., Bentinger, M., Zhao, A., Ansurudeen, I., Dallner, G., Catrina, S.-B., Brismar, K., Tekle, M., 2021. L-Carnosine Stimulation of Coenzyme Q10 Biosynthesis Promotes Improved Mitochondrial Function and Decreases Hepatic Steatosis in Diabetic Conditions. Antioxidants 10, 793. https://doi.org/10.3390/antiox10050793

Siqueira, J.S., Nakandakare-Maia, E.T., Vieira, T.A., Palacio, T.L.N., Grandini, N.A., Belin, M.A.F., Nai, G.A., Moreto, F., Altomare, A., Baron, G., Aldini, G., Francisqueti-Ferron, F.V., Correa, C.R., 2023. Effect of Bergamot Leaves (Citrus bergamia) in the Crosstalk between Adipose Tissue and Liver of Diet-Induced Obese Rats. Livers 3, 258–270. https://doi.org/10.3390/livers3020017

Siqueira, J.S., Vieira, T.A., Nakandakare-Maia, E.T., Palacio, T.L.N., Sarzi, F., Garcia, J.L., de Paula, B.H., Bazan, S.G.Z., Baron, G., Tucci, L., Janda, E., Altomare, A., Gado, F., Ferron, A.J.T., Aldini, G., Francisqueti-Ferron, F.V., Correa, C.R., 2022. Bergamot leaf extract treats cardiorenal metabolic syndrome and associated pathophysiological factors in rats fed with a high sugar fat diet. Mol. Cell. Endocrinol. 556, 111721. https://doi.org/10.1016/j.mce.2022.111721

Todisco, S., Santarsiero, A., Convertini, P., De Stefano, G., Gilio, M., Iacobazzi, V., Infantino, V., 2022. PPAR Alpha as a Metabolic Modulator of the Liver: Role in the Pathogenesis of Nonalcoholic Steatohepatitis (NASH). Biology (Basel). 11, 792. https://doi.org/10.3390/biology11050792

Vancells Lujan, P., Viñas Esmel, E., Sacanella Meseguer, E., 2021. Overview of non-alcoholic fatty liver disease (Nafld) and the role of sugary food consumption and other dietary components in its development. Nutrients 13. https://doi.org/10.3390/nu13051442

White, U., Ravussin, E., 2019. Dynamics of adipose tissue turnover in human metabolic health and disease. Diabetologia 62, 17–23. https://doi.org/10.1007/s00125-018-4732-x

Yang, D.K., Jo, D.G., 2018. Mulberry Fruit Extract Ameliorates Nonalcoholic Fatty Liver Disease (NAFLD) through Inhibition of Mitochondrial Oxidative Stress in Rats. Evidence-based Complement. Altern. Med. 2018. https://doi.org/10.1155/2018/8165716

Yılmaz, Z., Kalaz, E.B., Aydın, A.F., Soluk-Tekkeşin, M., Doğru-Abbasoğlu, S., Uysal, M., Koçak-Toker, N., 2017. The effect of carnosine on methylglyoxal-induced oxidative stress in rats. Arch. Physiol. Biochem. 123, 192–198. https://doi.org/10.1080/13813455.2017.1296468

Yki-Järvinen, H., Luukkonen, P.K., Hodson, L., Moore, J.B., 2021. Dietary carbohydrates and fats in nonalcoholic fatty liver disease. Nat. Rev. Gastroenterol. Hepatol. 18, 770–786. https://doi.org/10.1038/s41575-021-00472-y

Younossi, Z.M., Koenig, A.B., Abdelatif, D., Fazel, Y., Henry, L., Wymer, M., 2016. Global epidemiology of nonalcoholic fatty liver disease—Meta-analytic assessment of prevalence, incidence, and outcomes. Hepatology 64, 73–84. https://doi.org/10.1002/hep.28431

Highlights

- Consumption of high sugar-fat diets is related with MASLD,
- Carnosine improved lipid metabolism dysfunctions and oxidative stress in MASLD,
- Carnosine promoted modulation of PPAR-α mRNA expression,
- Carnosine can be effective for treating MASLD.

Table 1. Diet composition and nutritional values.

Components	Normocaloric	Hypercaloric
Soybean meal (g/kg)	335	340
Sorghum (g/kg)	278	80
Soy hulls (g/kg)	188,5	116,7
Dextrin (g/kg)	146,5	20
Maize starch (g/kg)	278	80
Sucrose (g/kg)	-	80
Fructose (g/kg)	-	180
Soybean oil (g/kg)	23	-
Lard (g/kg)	-	154,3
Minerals (g/kg)	25	25
Salt (g/kg)	4	4

Table 2. Nutritional characterization and obesity.

	Groups				Effects		
	Co	**Co+CAR**	**MAFLD**	**MAFLD+CAR**	**Diet**	**CAR**	**Interactions**
Food intake (g/day)	37.0 ± 2.31	36.3 ± 2.07	25.6 ± 0.904*	25.3 ± 1.72†	<0.001	0.528	0.858
Water intake (ml/day)	53.2 ± 3.79	52.0 ± 7.17	68.0 ± 4.02*	64.9 ± 3.48†	<0.001	0.320	0.564
Caloric intake (kcal/day)	133 ± 8.28	130 ± 7.42	166 ± 7.84*	168 ± 5.44†	<0.001	0.849	0.584
Initial body weight (g)	324 ± 25.0	324 ± 26.8	320 ± 16.4	314 ± 27.1	0.450	0.775	0.753
Final body weight (g)	502 ± 57.2	477 ± 25.8	569 ± 38.0*	530 ± 68.5	0.008	0.133	0.743
Weight gain (g)	145 ± 48.9	137 ± 23.2	250 ± 34.6*	198 ± 48.6†	<0.001	0.085	0.201
Adiposity index (%)	4.15 ± 1.60	3.12 ± 1.11	8.51 ± 1.03*	7.68 ± 2.56†	<0.001	0.19	0.883

Data are presented as mean ± standard deviation. Effects are the comparison by two-way ANOVA with Tukey's post-hoc test, with $p<0.05$ as statistically significance. Co: control group; Co+CAR: control group treated with carnosine; MASLD: MASLD induction group; MASLD+CAR: MASLD induction group treated with carnosine. * vs Co; † vs Co+CAR.

Table 3. Biochemical and hormonal markers.

	Groups				Effects		
	Co	**Co+CAR**	**MAFLD**	**MAFLD+CAR**	**Diet**	**CAR**	**Interactions**
AST (U/l)	155 ± 34.3	125 ± 18.6	114 ± 21.0	130 ± 32.4	0.128	0.532	0.058
ALT (U/l)	104 ± 14.4	69.5 ± 16.1*	83.0 ± 26.5	87.5 ± 21.5	0.858	0.084	0.028
Uric acid (mg/dl)	0.967 ± 0.175	0.800 ± 0.420	1.27 ± 0.761	1.67 ± 1.69	0.150	0.768	0.476
Urea (mg/dl)	58.8 ± 8.66	61.0 ± 9.63	35.0 ± 15.5*	44.2 ± 4.58†	<0.001	0.195	0.417
Creatinine (mg/dl)	4.48 ± 3.08	4.59 ± 5.01	4.48 ± 1.68	4.36 ± 0.985	0.931	0.998	0.930
Blood Glucose (mg/dl)	78.0 ± 8.29	86.3 ± 11.4	88.8 ± 6.74*	97.3 ± 4.50†	0.004	0.020	0.980
Total Cholesterol (mg/dl)	62.3 ± 7.12	46.5 ± 10.1*	52.7 ± 9.63	62.0 ± 8.32†	0.430	0.380	0.002
Triglycerides (mg/dl)	70.4 ± 16.9	41.0 ± 8.32*	205 ± 34.6*	112 ± 27.4#†	<0.001	<0.001	0.004
HDL (mg/dl)	14.5 ± 3.02	14.0 ± 1.79	11.4 ± 2.33	15.5 ± 3.27#	0.471	0.114	0.047
n-HDL (mg/dl)	47.8 ± 4.67	40.5 ± 10.9	40.2 ± 6.59	46.5 ± 5.79	0.785	0.870	0.035
Insulin (ng/ml)	0.224 ± 0.031	0.175 ± 0.039	0.306 ± 0.039*	0.293 ± 0.073†	<0.001	0.132	0.379
HOMA - IR	1.24 ± 0.199	1.07 ± 0.227	1.93 ± 0.304*	2.03 ± 0.535†	<0.001	0.800	0.342

Data are presented as mean ± standard deviation. Effects are the comparison by two-way ANOVA with Tukey's post-hoc test, with $p<0.05$ as statistically significance. Co: control group; Co+CAR: control group treated with carnosine; MASLD: MASLD induction group; MASLD+CAR: MASLD induction group treated with carnosine; AST: aspartate aminotransferase; ALT: alanine aminotransferase; HDL: high density lipoprotein; n-HDL: non-high-density lipoprotein; HOMA-IR: homeostasis model assessment – insulin resistance. * vs Co; # vs MASLD; † vs Co+CAR.

Figure

Click here to access/download;Figure;Figure 1.jpg

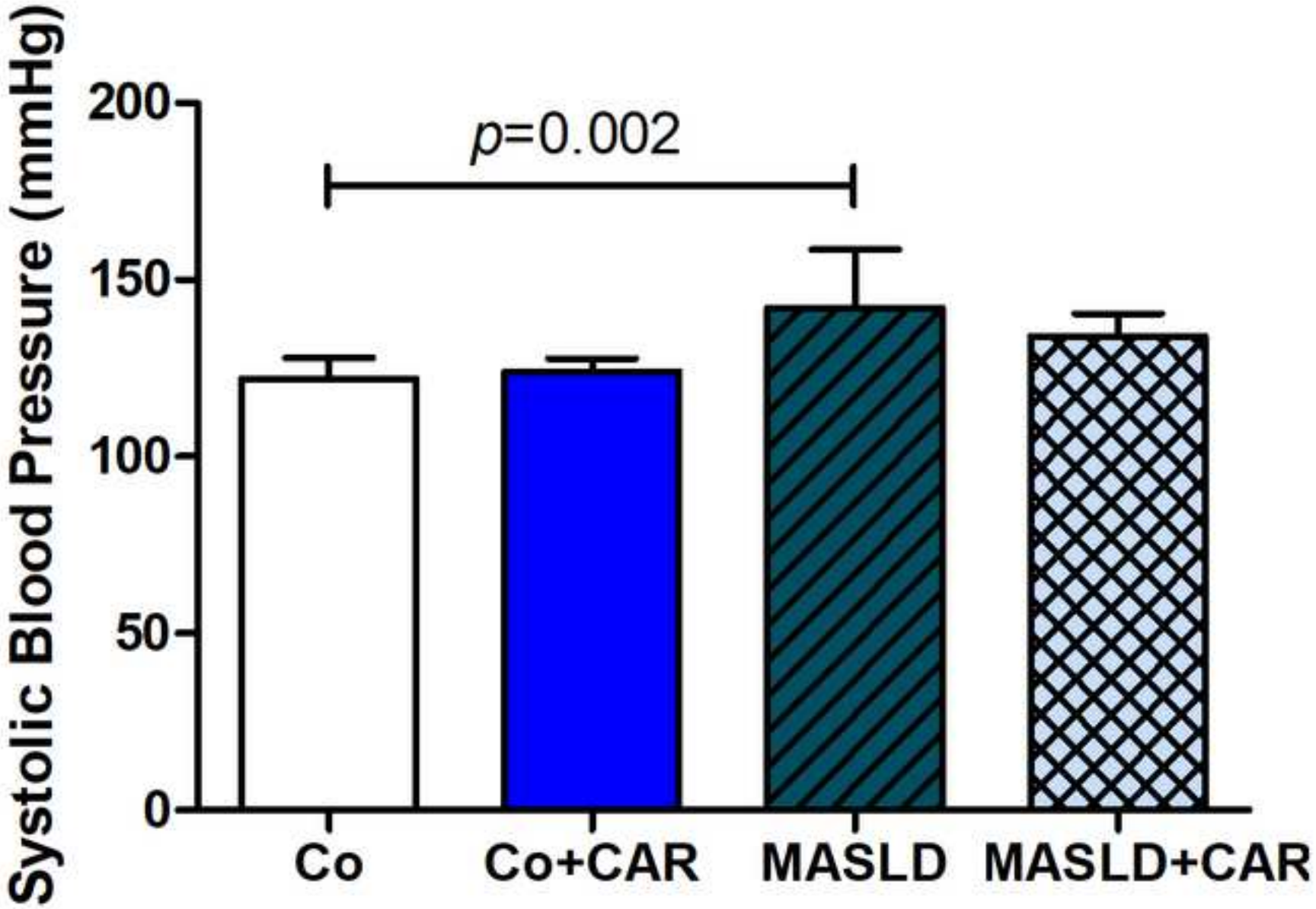

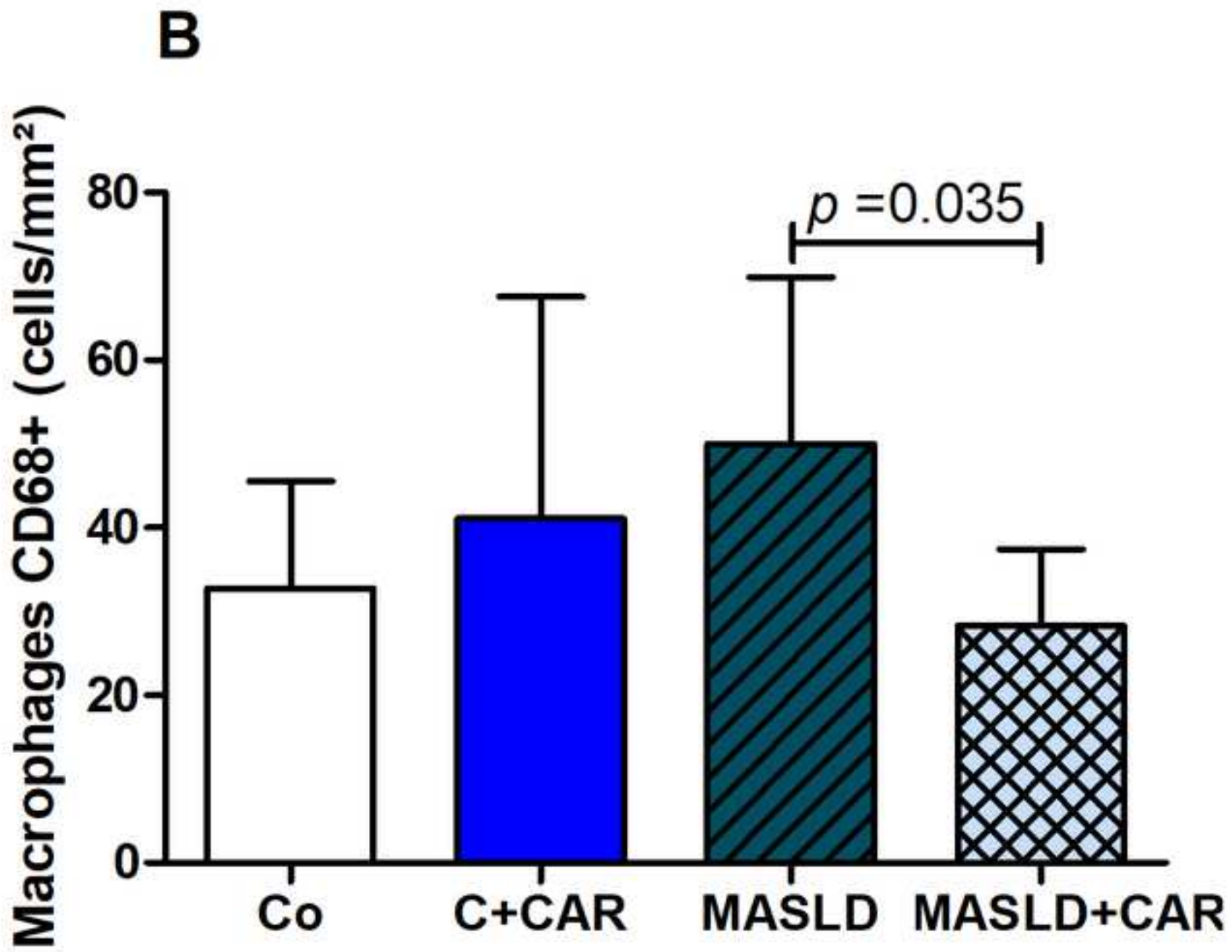

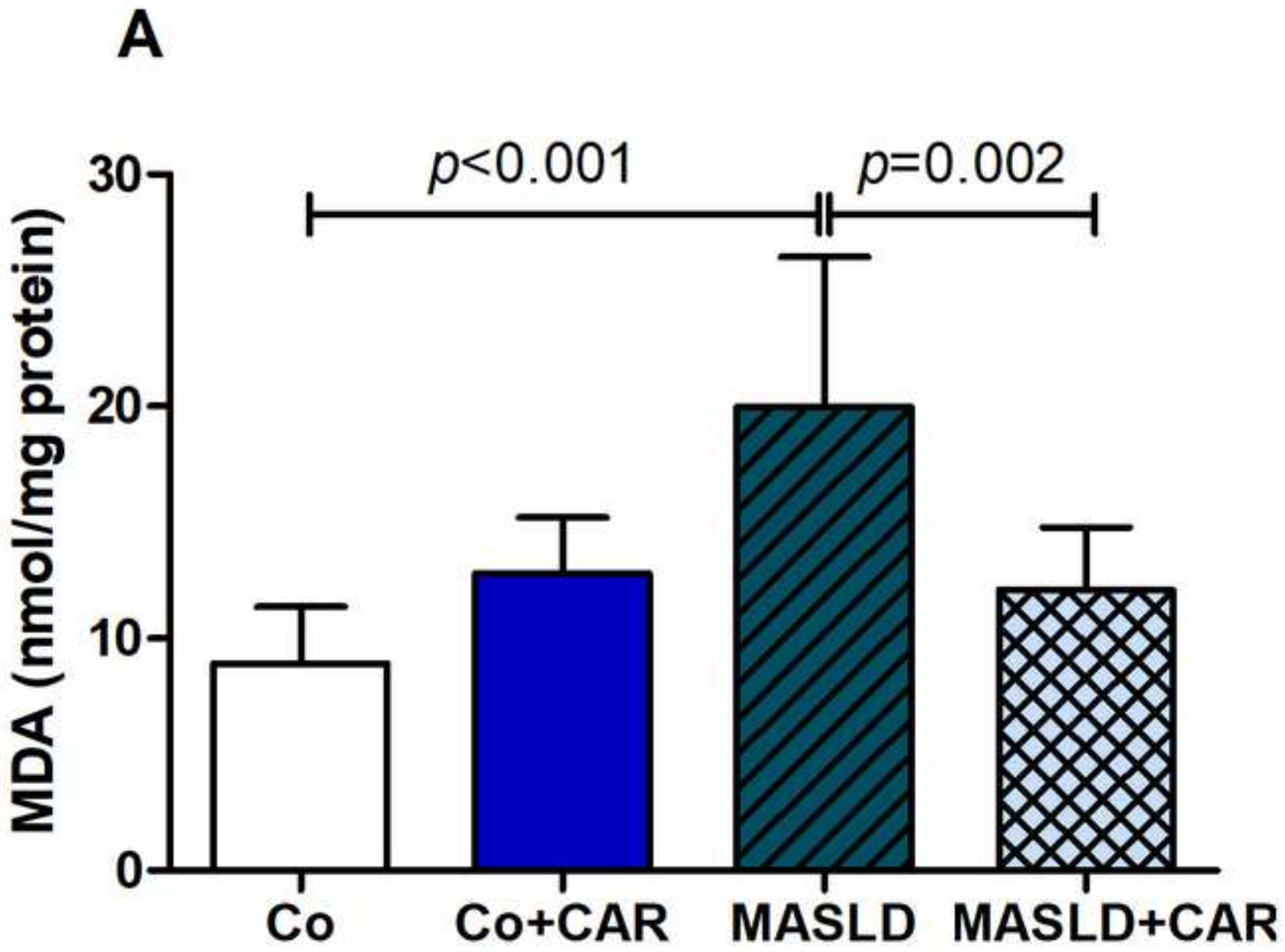

Figure

Click here to access/download;Figure;Figure 4B.jpg

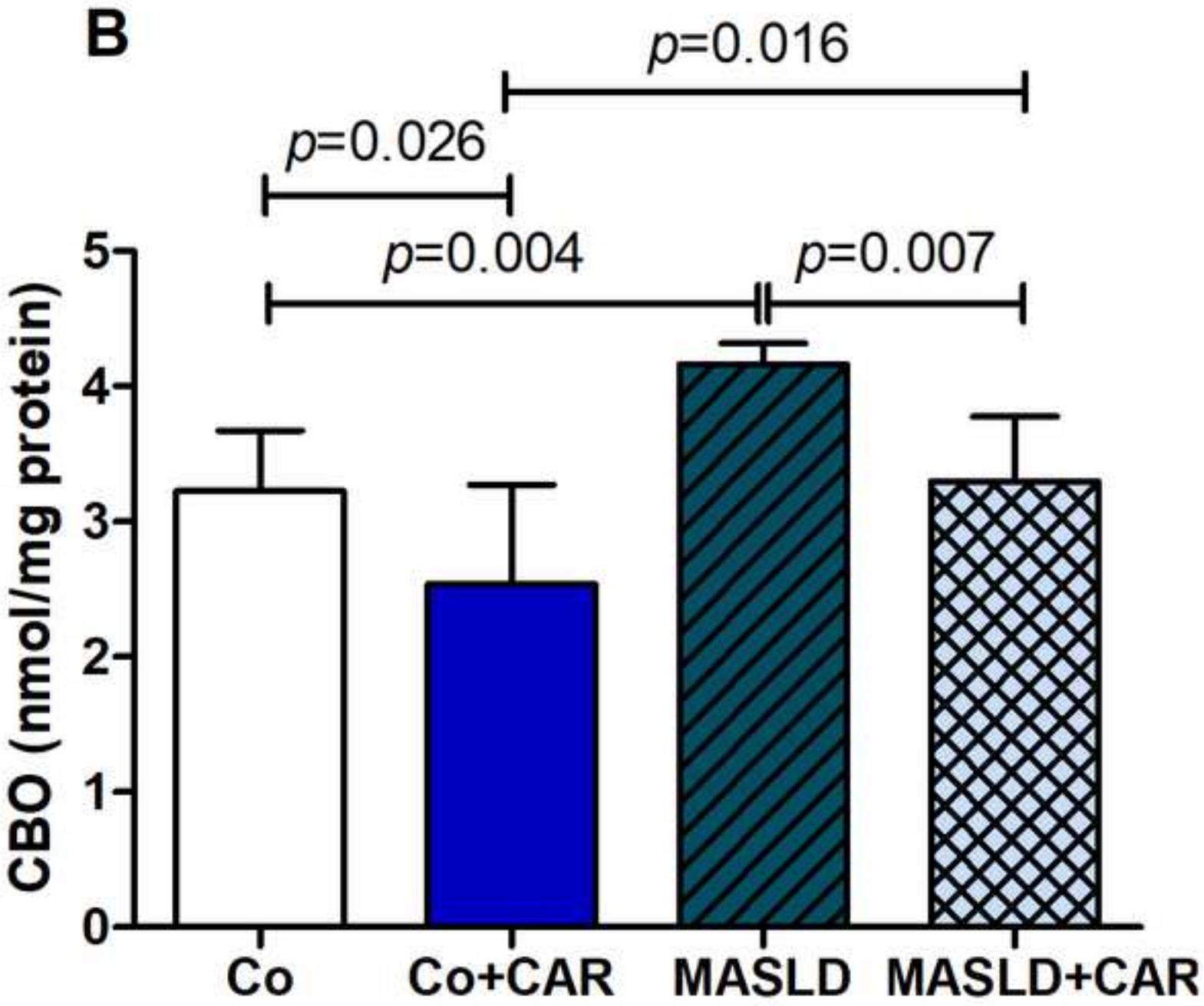

Figure

Click here to access/download;Figure;Figure 5A.jpg

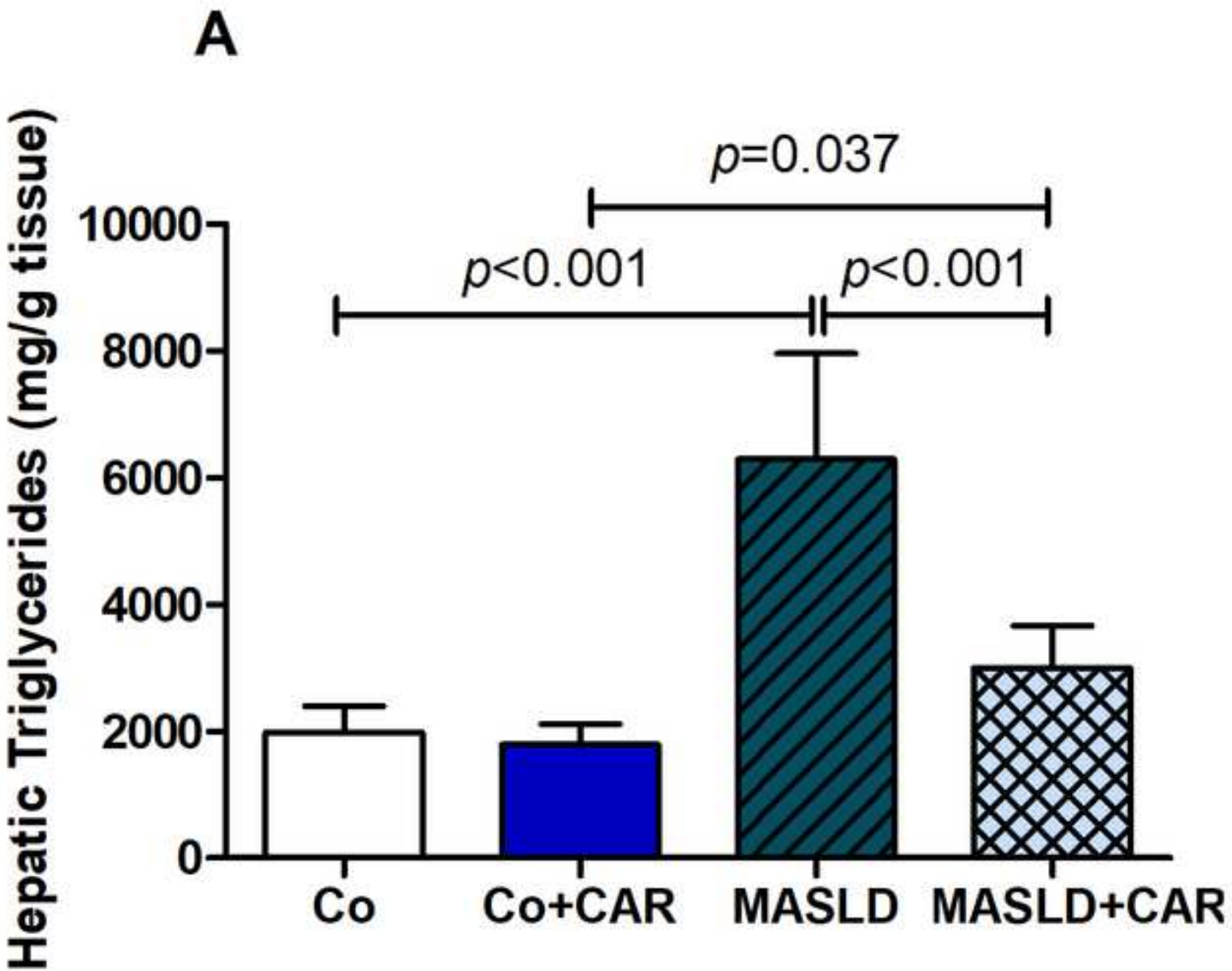

Figure

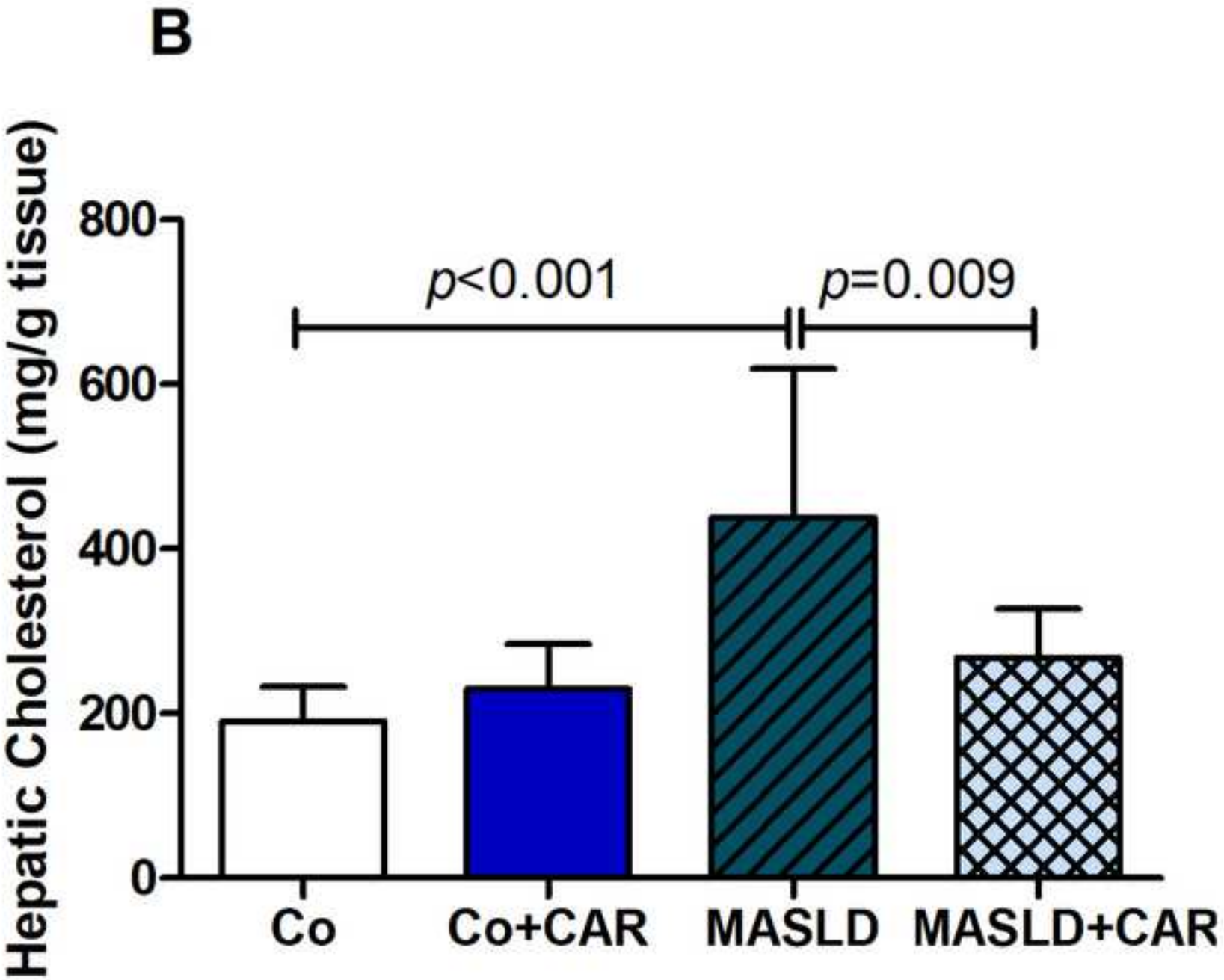

Figure

Click here to access/download;Figure;Figure 6A.jpg

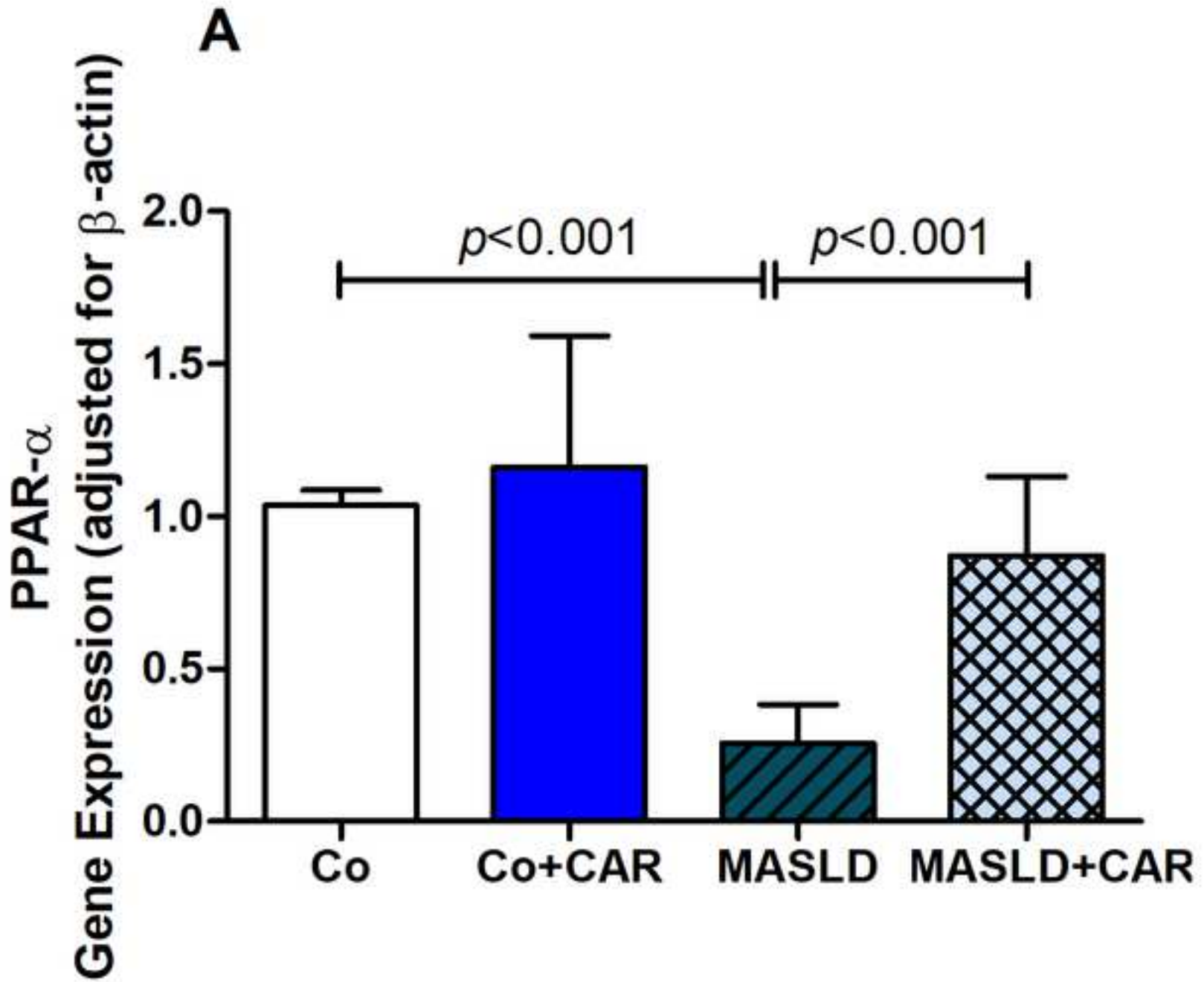

Figure

Click here to access/download;Figure;Figure 3A.jpg

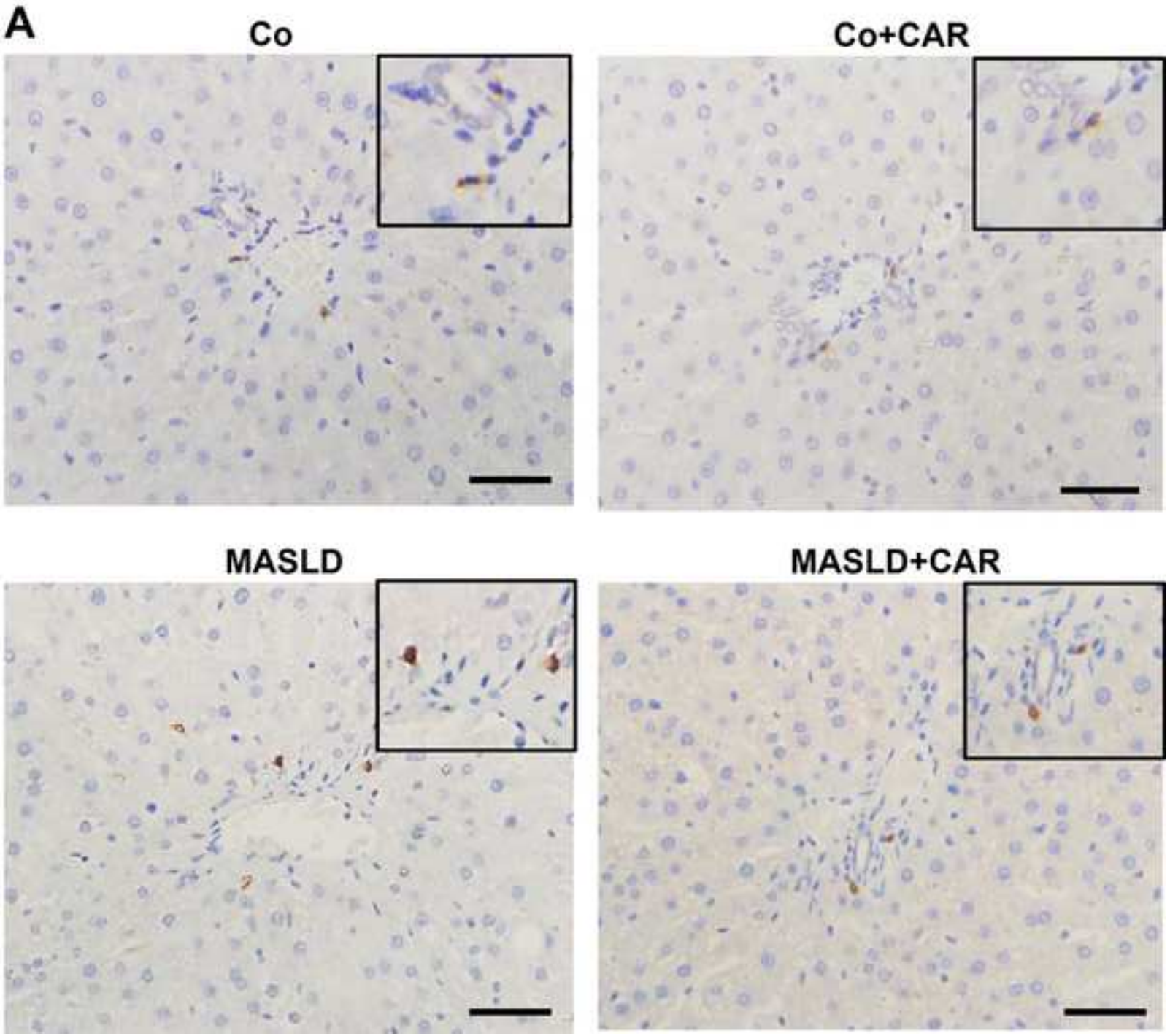

Figure

Click here to access/download;Figure;Figure 4C.jpg

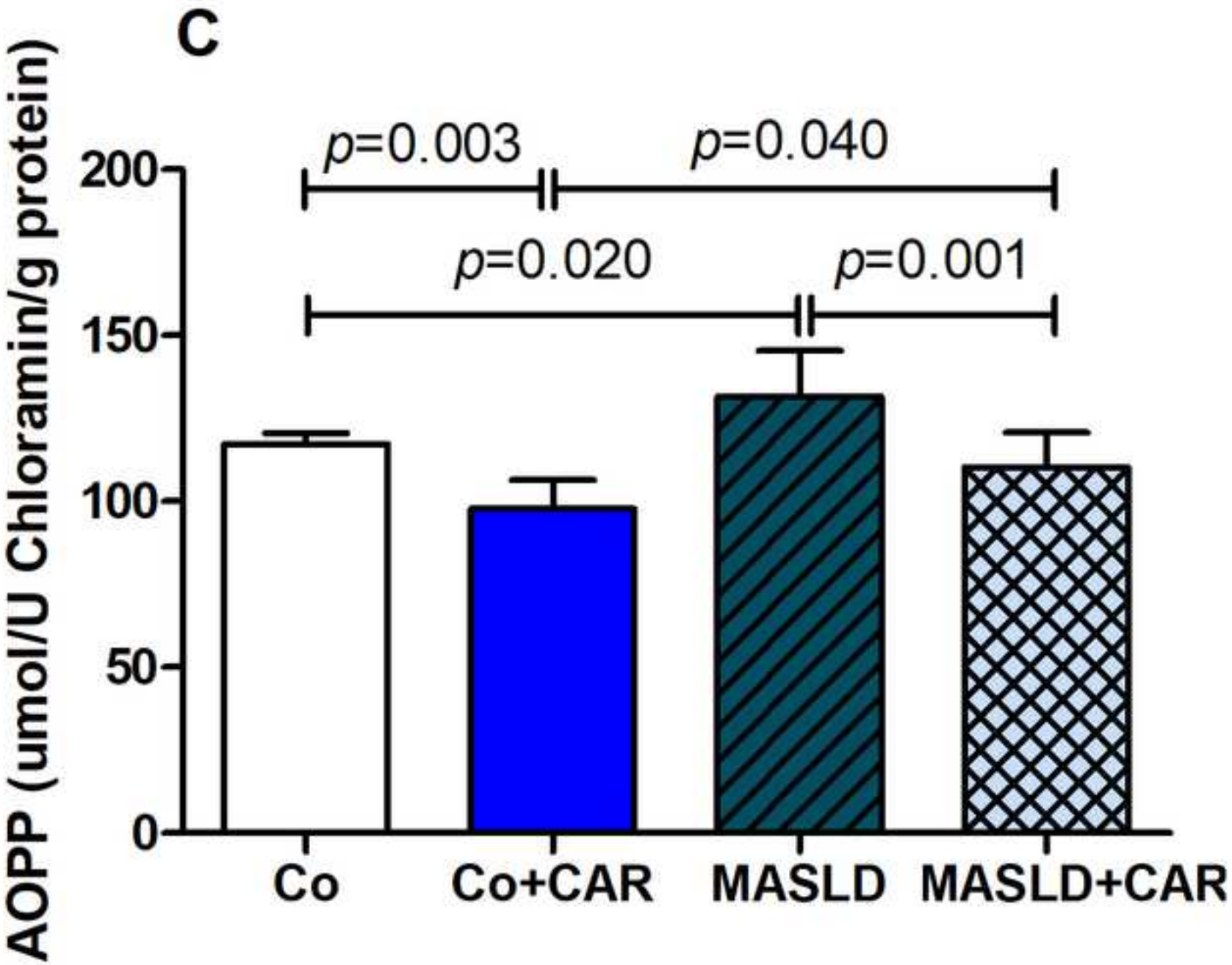

Figure

Click here to access/download;Figure;Figure 2 new.jpg

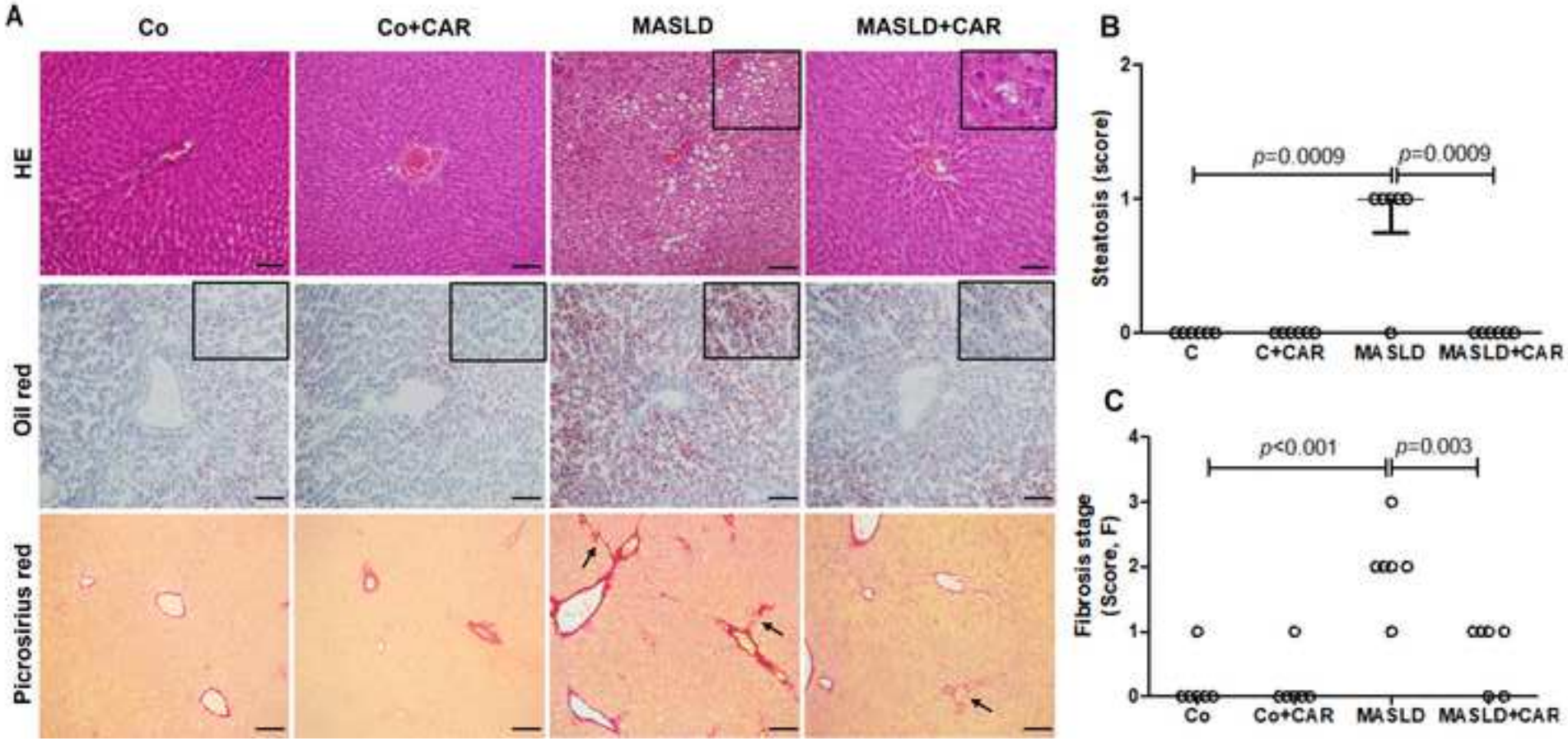

Figure